Please cite this article in press as: Lu et al., The timescale identification decoupling complicated kinetic processes in lithium batteries, Joule (2022), https://doi.org/10.1016/j.joule.2022.05.005

Joule

CellPress

Perspective

The timescale identification decoupling complicated kinetic processes in lithium batteries

Yang Lu,[1] Chen-Zi Zhao,[1,3,*] Jia-Qi Huang,[2] and Qiang Zhang[1,*]

SUMMARY

A comprehensive understanding of multiple Li kinetics in batteries is essential to break the limitations of mechanism study and materials design. Various kinetic processes with specific relaxation features can be clearly identified in timescales. Extracting and analyzing the timescale information in batteries will provide insights into investigating kinetic issues such as ionic conductions, charge transfer, diffusions, interfacial evolutions, and other unknown kinetic processes. In this regard, the timescale identification is an important method to combine with the non-destructive impedance characterizations in length scale for online battery monitoring. This perspective introduces and advocates the timescale characterization in the views of the basic timescale property in batteries, employing the concept of distribution of relaxation time (DRT) and presenting successful applications for battery diagnosis. In the future, we suggest that timescale characterizations will become powerful tools for data extraction and dataset building for various battery systems, which can realize data-driven machine learning modeling for practical application situations such as retired battery rapid sorting and battery status estimations.

INTRODUCTION

Rechargeable lithium batteries have been treated as an important section of clean energy networks to realize carbon neutralization.[1,2] Contemporary secondary batteries have become indispensable sections of our daily life. Increasing demands for energy storage promote the development of lithium batteries and the exploration of next-generation energy storage systems, such as Li-S batteries, metal-air batteries, and solid-state batteries with enhanced energy density and safety.[3,4] There are complicated electrochemical processes within battery systems, which play a crucial role in battery cycling but are difficult to identify.[5–7] Hence, it is a big challenge to clarify the Li kinetics, especially for the next-generation battery systems.

Different kinetics processes are exhibiting their specific relaxation times within the battery systems, offering great opportunities to distinguish and quantify the multi-scaled characteristics.[8] Acquiring length-scaled material information requires dissembling the batteries, which is destructive analysis. The timescale-based kinetic properties such as ionic transport, charge transfer, and diffusion can be monitored in a non-destructive way.[9] Extracting accurate timescale parameters is fundamental to quantifying the battery kinetics, which can be applied to monitor battery status during continuous operations.[10] It is essential to build the battery management system (BMS) and estimate the state of charge (SOC), the lifespan of batteries, and more possible evaluation for practical batteries.[11] Hence, timescale-based studies possess both academic and practical values.

Context & scale

Characterizations from different scales are powerful to unravel the hidden mechanisms of working batteries. The timescale diagnosis is an emerging strategy to disassemble the battery "black box" into isolated kinetic information, which not only contributes to a non-destructive practical battery test but also helps to decouple and quantify Li kinetics in-time dimensions such as interfacial properties, ion transportation, and charge transfer processes. This paper introduces the basic scientific knowledge, protocols, applications, and outlooks on the rapidly developing timescale analyses in various battery systems, such as solid-state batteries, metal-S/O_2 batteries, and metal-ion batteries. We hope the fresh viewpoint can help to popularize the timescale analyses in both academic study and industry applications.

These kinetics characteristics are conveyed by the possible ionic double layer existing in various heterogeneous interfaces, such as grain boundary, solid-electrolyte interphase, electrode-electrolyte contact, interfacial charge transfer, etc. The timescale kinetic properties are determined by intrinsic materials structure (e.g., solid-state electrolyte and electrode materials), the interfacial characters (e.g., components in solid-electrolyte interphases), the battery systems (e.g., batteries with solid-state electrolytes and liquid electrolytes), and dominated ionic carriers (e.g., Li ions, Na ions, oxygen ions, etc.).[12] The external loading will change the steady state of each component in batteries. Their current-induced responses will lead to the discrepancy of relaxation, reflected as the specific time constants.[13] The alternating current (AC) electrochemical impedance spectroscopy (EIS) is a powerful characterization method to unravel the electrochemical process in timescale.[14]

EIS is indispensable for battery diagnoses due to the advantages such as high accuracy and non-destructive feature to investigate the black-box systems. As evaluated, each electrochemical process can be described by specific circuit element combinations such as resistances, capacitances, and inductances. The EIS spectra are usually interpreted by the conventional equivalent circuit model (ECM) method to simulate the real situation in battery systems. According to the circuit model, the specific electrochemistry processes can be distinguished and quantified as interfacial contact, charge transfer process, diffusion, etc. The Randles circuit (RC paralleled circuit) is a typical model to simulate the interfacial process consisting of ionic double layer and transport resistances. Herein, a time constant of this Randles circuit is ensured as $\tau = RC = \frac{1}{2\pi f}$. The distinguished time constant and specific frequency represents a single process in the electrochemical system. Hence, the accurate timescale modeling of a battery is essential to kinetics interpretation. At present, modeling the battery system is mainly an experience-dependent study by identifying the semi-circle or frequency or obeying the correlated experienced knowledge. If some specific electrochemistry processes possess similar time constants, their EIS responses may be coupled together, which will import difficulties in constructing the equivalent circuit. The conventional experience-dependent ECM will result in the misunderstanding of the battery analyses due to the lumped-parameter characteristics of the battery systems. An EIS result can fit more than one ECM. Ensuring all the time constants in the whole electrochemistry system is the precondition for accurate battery modeling. The distribution of relaxation times (DRT) can directly distinguish the time constant of the major electrochemistry process, which can simplify the impedance analyses and significantly improve the accuracy of kinetics interpretation in the timescale.[15,16] It is noticed that DRT concepts are becoming promising techniques for being applied in energy storage areas, including various battery mechanism studies,[17,18] materials evaluations,[19–21] battery status predictions,[22] etc. Furthermore, the timescale characterization is a digital method with physical measurement and mathematical treatment, which is suitable for data-driven analyses and interdisciplinarity studies.[23] This perspective aims to provide insights on quantifying the kinetics by DRT method which is based on timescale analysis.

TIMESCALE EXHIBITIONS

The timescale effects in battery systems are mainly derived from four basic physical processes: electric double layer, local charge concentration, charge equilibrium, and concentration gradient in electrolyte or electrode materials.[24] The external stimulations (e.g., current or voltage) can induce the relaxation processes of different physical situations. Relaxation means the recovery processes after the external interferences, which are intrinsic properties of one isolated system. Consequently,

[1]Beijing Key Laboratory of Green Chemical Reaction Engineering and Technology, Department of Chemical Engineering, Tsinghua University, Beijing 100084, China

[2]Advanced Research Institute of Multidisciplinary Science, Beijing Institute of Technology, Beijing 100081, China

[3]State Key Laboratory of Automotive Safety and Energy, School of Vehicle and Mobility, Tsinghua University, Beijing 100084, China

*Correspondence:
zcz@mail.tsinghua.edu.cn (C.-Z.Z.),
zhang-qiang@mails.tsinghua.edu.cn (Q.Z.)

https://doi.org/10.1016/j.joule.2022.05.005

Please cite this article in press as: Lu et al., The timescale identification decoupling complicated kinetic processes in lithium batteries, Joule (2022), https://doi.org/10.1016/j.joule.2022.05.005

different relaxation properties can be used to distinguish the kinetics processes in the batteries, distinguishing the Li-ion conduction, adsorption, and release on the interfaces. This timescale exhibition is an emerging powerful strategy to investigate the kinetics in battery systems quantitatively, which is also an extension for conventional EIS tests. Hence, an accurate definition of all the time constants is the prerequisite, which requires the identification of the DRT in the electrochemical systems.

The fundamentals of DRT

The concept of DRT is firstly put forward by Schweilder et al. in 1907.[25] The electrochemical system is mainly measured and displayed in the frequency domain. The target of the DRT is to transform the timescale characteristics of frequency-based EIS in the time domain. It is an effective assumption to simulate the convergent impedance of the electrochemistry system as the series connection of Ohm impedance (R_0) with polarization impedance (R_{pol}, $Z_{pol}(f)$) induced by electrochemical processes.[15] The $Z_{pol}(f)$ is decomposed as a continuous series connection of RC paralleled circuit to represent the evolved electrochemical and physical processes in the DRT method. Hence, the pre-modeling of ECM can be avoided. Considering the existence of inductance (L_0), the total circuit is displayed as

$$Z(f) = R_0 + i2\pi f L_0 + Z_{pol}(f) \quad \text{(Equation 1)}$$

A typical RC paralleled circuit satisfies a relationship of $RC = \tau^*$, where τ^* represents the time constant of this RC paralleled circuit. The impedance of each typical RC paralleled circuit is calculated as $\frac{R_x}{1+j\omega\tau}$. If each R_x is described by relaxation distribution function $g(\tau_x)$ with a time constant of τ_x in timescale, after extracting the polarization impedance R_p, the transition relationship between frequency domain $Z(f)$ and time domain $g(\tau)$ is displayed as:[26,27]

$$Z(f) = R_0 + i2\pi f L_0 + R_p \int_0^\infty \frac{g(\tau)}{1+i2\pi f\tau} d\tau \quad \text{(Equation 2)}$$

$$\int_0^\infty g(\tau) d\tau = 1 \quad \text{(Equation 3)}$$

The inductance can be eliminated as a conventional DRT equation:

$$Z(f) = R_0 + R_p \int_0^\infty \frac{g(\tau)}{1+i2\pi f\tau} d\tau \quad \text{(Equation 4)}$$

Actually, the EIS frequencies are usually measured and shown logarithmically. Hence, the time constant is also displayed in logarithmic coordinates, which can be written as[27,28]

$$Z(f) = R_0 + R_p \int_0^\infty \frac{\gamma(\ln\tau)}{1+i2\pi f\tau} d\ln\tau \quad \text{(Equation 5)}$$

$$\gamma(\tau) = \tau g(\tau) \quad \text{(Equation 6)}$$

The $g(\tau)$ is calculated numerically, where the integral type in the equation can be written in the finite sum.[29]

$$Z(f) = R_0 + R_p \sum_{k=1}^{n} \frac{g(\tau_k)}{1+i2\pi f\tau_k} \quad \text{(Equation 7)}$$

$$\sum_{k=1}^{n} g(\tau_k) = 1 \quad \text{(Equation 8)}$$

These equations are fundamental for DRT methods, and the deconvolution toward EIS as $g(\tau)$ is the core issue during data analysis. Many methods have been applied to

Please cite this article in press as: Lu et al., The timescale identification decoupling complicated kinetic processes in lithium batteries, Joule (2022), https://doi.org/10.1016/j.joule.2022.05.005

explore the solutions of $g(\tau)$. Various types of algorithms have been developed at MATLAB, Python, or self-created software plateaus to satisfy the DRT practices for EIS deconvolution.

The DRT can be accomplished by Fourier transform,[30] Monte Carlo sampling,[31] maximum entropy,[32] fractional algebraic identification,[33] and the most popular Tikhonov regularization strategy.[26] Many new solutions such as the Gaussian process[34] and genetic programming[35] are both efficient solutions to realize the DRT deconvolution. Some typical methods are introduced as follows.

The Tikhonov regularization

The DRT is realized by the calculation of the distribution function, which is an ill-posed problem. Tikhonov regularization (also known as ridge regression) is one of the most popular and effective solutions that are parameter dependent. In the regularization process, the noisy data are smoothed by adding an extra penalty term to the least square regression. Considering the quality of data, the penalty term is weighted by the regularization parameter (λ). Hence, the optimization function is also written as:[36,37]

$$\min_x F_\lambda = \underbrace{\|Ax - y\|^2}_{\text{least squares}} + \underbrace{\lambda \|x\|^2}_{\text{penalty}}, \qquad \text{(Equation 9)}$$

The regularization parameters (λ) determine both the smoothness and resolution of the DRT results. Generally, the high regularization parameter will result in a smooth and wide peak, suppressing the erroneous oscillations and preventing data over interpretation (overfitting), but the resolution may be deteriorated, leading to the miss of effective information (underfitting). In contrast, the low regularization parameter shrinks the peak width and the peak will become sharp. The decreased λ can realize the separation of the peaks and increase the time-domain resolution. However, the extremely low λ will result in the oscillation and the pseudo peaks (overfitting), which will lead to a misunderstanding of the EIS spectra. The high regularization parameter suppresses the oscillation and the low parameter increases the resolution. Hence, the regularization parameter is crucial to provide accurate time-domain interpretation.

Typical DRT still relies on the pre-setting regularization parameters. However, some emerging methods have realized the parameter free or automatic parameter tuning during DRT analyses. Zhang et al. developed a new Tikhonov approach-based algorithm that is free of finding parameters to rebuild the DRT function.[38] Their methods enable the elimination of the pseudo peaks and solve the discontinuity in the DRT, which provides excellent precision for DRT analyses. Žic et al. developed the Levenberg-Marquardt algorithm (LMA) for computing the DRT by automatically updating the regularization parameter.[39]

Impedance spectroscopy genetic programming (ISGP) method

The genetic programming for the DRT solution is developed by Tsur's team, which is named impedance spectroscopy genetic programming (ISGP).[35,40] The ISGP chooses amounts of distribution functions and random parameters to form the "genetic pool." The fitness from each combo of function and parameter is tested and compares the fitted reconstructed impedance with the measured results. After scoring the fitness result, the optimized parameter and function are screened. The new generation evolves from the cross over by the genes and the random mutations, then the new generation is scored subsequently. This optimization is

Please cite this article in press as: Lu et al., The timescale identification decoupling complicated kinetic processes in lithium batteries, Joule (2022), https://doi.org/10.1016/j.joule.2022.05.005

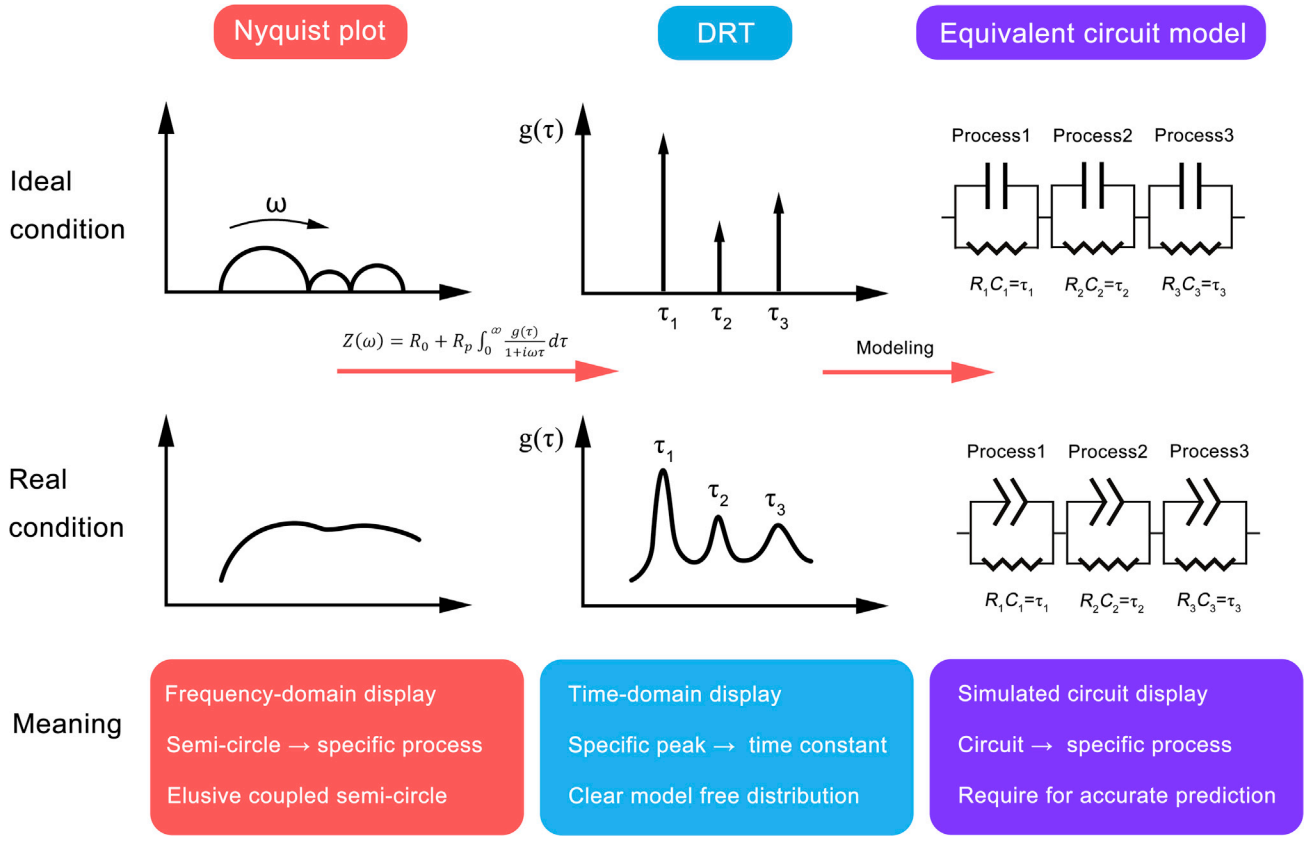

Figure 1. The relationship among the EIS based Nyquist plots, ideal equivalent circuit models, and real condition electrochemical models

continued until the highest fitness score to acquire the distribution function and the optimized parameter.

Gaussian process DRT

The deconvolution for DRT from experimental EIS datasets is an ill-posed problem, which is sensitive to the data noise. The widely used regularization method for DRT such as ridge regression requires the manual selection of hyperparameters (regularization parameter), which will import subjectivity for data analyses. The pre-screening for hyperparameter is essential to obtain accurate time-domain analyses in DRT. Except for designing the parameter screening steps, deconvolution on DRT can be developed by a brand new method such as assuming the DRT as a Gaussian process (GP) to replace the regularization. The parameter defining the GP-DRT model can be selected, maximizing the experimental evidence. The Gaussian method enables the management of the data noise, overlapped timescale feature, incontinuous data, and inductive characteristics in the probabilistic view, which overcomes the limitations of the conventional DRT by regularization.[34] The finite Gaussian process DRT (fGP-DRT) inherits the advantages of GP-DRT and breaks the limitation on constraining to produce non-negative DRT and using both the real and imaginary parts of the EIS.[41]

Relations between the DRT and equivalent circuit model

The relationships among Nyquist plots, the DRT plots, and the ECM are displayed in Figure 1. Ideally, a typical EIS is composed of separated semicircles. Each semi-circle

Please cite this article in press as: Lu et al., The timescale identification decoupling complicated kinetic processes in lithium batteries, Joule (2022), https://doi.org/10.1016/j.joule.2022.05.005

is related to a specific time constant, which can be exhibited as isolated straight lines in DRT plots, corresponding to respective paralleled circuits of resistance and capacitor. Practically, the semicircles in EIS plots are intercoupling and hard to distinguish, and the DRT can transform the coupled EIS as continuous curves with several specific peaks, which represent the constant phase elements (CPE) influenced paralleled capacitor and resistance. The specific time constants can also be identified by the center of the peaks. The related ECM model can also be acquired according to the deconvoluted time constants.

The DRT has been widely used in solid oxide fuel cells (SOFC) to identify and understand the key kinetics processes such as mass transport and reaction in electrodes and the interfaces.[42–44] Its application in ion or metal batteries is still at the seedling stage. The emergence of new battery systems such as Li-S batteries, solid-state batteries, Al-ion, and Zn-ion batteries are developing rapidly, which will possess their unique detailed electrochemistry characteristics.

Solutions for non-convergence DRT

The EIS in SOFC exhibiting the convergence feature can be successfully decomposed along with the EIS of the battery system at high and middle-frequency parts. However, the typical non-convergence EIS is common in the low-frequency part of a battery system. The pure capacitive tail in EIS cannot be described as typical RC paralleled models, which is the methodical limitation of DRT methods for interpreting battery systems.

The EIS in battery with diffusion capacitive information (C_{DC}) can be modified based on DRT models:[45]

$$Z(f) = R_0 + R_P \int_0^{\infty} \frac{g(\tau)}{1 + i2\pi f\tau} d\tau + \frac{1}{i2\pi f C_{DC}} \qquad \text{(Equation 10)}$$

After solving the RC parts by DRT, the differential parts can be solved by the distribution function of differential capacity (DDC) method, the distribution of diffusion times (DDT) method, etc.[45,46] The low-frequency non-convergence part such as the differential capacitive tail in EIS is assumed as the aggregation of the convergent complex capacitive. The timescale features can also be decomposed by a distribution function, where the DDC is defined as:[47]

$$C(f) = C_{diff} \int_0^{\infty} \frac{h(\tau)}{1 + i2\pi f\tau} d\tau \qquad \text{(Equation 11)}$$

Where C_{diff} is the total differential capacity and $h(\tau)$ represents the distribution function of differential capacitance.

Using a similar deconvolution method as that in the DRT method, the timescale information differential capacitive information can be achieved, which is one of the powerful complementary methods for timescale analyses. The DDT is another potential solution for the non-convergence EIS.[46] The DDT theory connects the distribution of diffusion time with the specific electrochemistry system, which can help to unravel the diffusion, transport pathways, and geometrical information in the battery system. This model assumes that the electrochemistry processes contribute as independent diffusion pathways in parallel with different diffusion times. Hence, the model is given as:

$$\frac{1}{Z(f)} = \int_0^{\infty} \frac{P(\tau)}{Z_D(f, \tau)} d\tau \qquad \text{(Equation 12)}$$

Please cite this article in press as: Lu et al., The timescale identification decoupling complicated kinetic processes in lithium batteries, Joule (2022), https://doi.org/10.1016/j.joule.2022.05.005

Where $P(\tau)$ is the DDT and Z_D derived from the finite-length diffusion model. In the geometrical view, the diffusion time $\tau = L^2/D$ is related to the diffusion path length L and diffusivity D, which provides the possibility to build an "impedance imaging" for the nanostructures by transforming the EIS to the $P(\tau)$. The mathematical transformation can also be solved by Tikhonov regularization, Lasso regularization Fourier transformation, etc. The DDT model not only can be used to demonstrate the pure diffusion process but also can be utilized in the reaction-diffusion situations, which is described by the Gerischer circuit elements. Hence, this method can also help to supplement the DRT in the entire frequency region and can even work as an emerging method to individually study the impedance. The conventional DDT is based on the assumption of thin electrodes that obey the $\tau = L^2/D$. Ciucci's group developed the non-linear DDT (NL-DDT), which extends the DDT method to include the high frequency in the thick electrode system, widening the application scenarios in various electrochemistry systems.[48] Until now, DDT has not been widely applied in analyzing battery systems. Combined with the DRT technique, the DDT is also promising the promote accurate EIS interpretation.

The superiority of DRT in timescale analyses

The DRT is a model-free method, which avoids the pre-modeling of the electrochemistry system and can display clear time-domain characteristics. Conventional electrochemical analyses of EIS in battery systems relied on the model based on experiences and might lose novel electrochemistry details. EIS as one of the most important electrochemistry methods can acquire abundant internal information combined with *in situ* galvanostatic electrochemical impedance spectra. An accurate interpretation of EIS is essential. The DRT is a promising solution to further analyze the EIS. Basically, the DRT can avoid the erroneous ECM pre-modeling, which leads to possible misunderstandings. Considering the complexity of battery systems, the superiorities of DRT toward battery diagnosis are listed below.

Increased resolution compared with conventional analyses

ECM and identifying from Bode plots are conventional methods for EIS interpretation. However, both of them have fallen behind compared with DRT. Professor Ouyang Minggao's team compared the ECM method and DRT method in the SOFC system, they proved that ECM will lose some processes and DRT can accurately determine them.[49] Bode plots can provide frequency-based information to identify different electrochemistry processes. However, the resolution of Bode plots is still limited. As reported by Huang et al., the frequency-based resolution of Bode plots can only separate the processes in a simple model with similar intensity and obvious frequency differences for over 10 times.[50] Hence, considering the complex electrochemistry system, if more kinetics processes with approached time constants are involved, the resolution of Bode plots cannot satisfy the demands and some processes with weak intensity will be missed. For example, as shown by Kim et al., DRT results exhibit an obviously increased resolution at frequency scale, which helps to quantify the impedance for four kinetics processes in SOFC.[51] Timescale information in battery systems is more complex with anodic, cathodic, and electrolyte information, which is more appropriate for DRT.

Visualizing the quantifying the complex electrochemical processes

Different peaks in DRT plots can be clearly identified to present the electrochemical processes, providing much more information compared with coupled Nyquist plots. The impedance of various processes can be quantified based on the peaks located at different timescales. Some batteries are operated accompanying a series of kinetics processes (e.g., Li-S batteries), which possess different kinetics

Please cite this article in press as: Lu et al., The timescale identification decoupling complicated kinetic processes in lithium batteries, Joule (2022), https://doi.org/10.1016/j.joule.2022.05.005

procedures with similar time constants. That will result in the coupled semicircles in Nyquist plots, which is challenging to distribute these kinetics processes. DRT can accurately distinguish different electrochemical processes according to the time constants.

Analyzing the batteries with ultra-low total impedance

The conventional manual simulation of different ECMs might result in severe errors when the batteries exhibit low total impedance (e.g., high capacity pouch cell and battery mold), whereas DRT methods can accurately quantify the impedance of a specific electrochemical process due to the independence of circuit models.

In situ monitoring dynamic evolutions

The *in situ* galvanostatic electrochemical impedance spectra (GEIS) is an emerging method to monitor the electrochemistry evolution during continuous cycling, which is important to unravel the hidden kinetic mechanisms. The GEIS measurements will produce a series of impedance results. Manual simulations for many *in situ* impedance results are time consuming and will lose the *in situ* data accuracy due to the uncontrollable manual errors. DRT is based on algorithm calculation, which can batch process the EIS data, guaranteeing accuracy and efficiency.

TIMESCALE DIAGNOSIS

Distributing the time constant of a typical electrochemical process is the priority for the EIS study. Identifying their timescale is fundamental to EIS interpretation. The typical workflow for DRT diagnosis in battery research is shown in Figure 2.

The typical procedure for battery diagnoses by DRT

Measuring and pre-processing for DRT

The DRT diagnosis is started by EIS measurement with wide frequency. The accuracy of EIS will determine the DRT results. Hence, the validity test of the EIS result is essential. Accurate time-domain analyses by DRT require high-quality EIS data with a high signal-to-noise ratio. The noisy data in EIS will lead to pseudo peaks during the regularization for DRT, which can result in the misunderstanding of the electrochemistry model.[52,53] Hence, the validity of the EIS data should be pre-certified before further analyses. The most frequently used criterion is the Kramers-Kronig transformation. If the frequency-dependent impedances satisfy the linearity and the time invariance, the real and imaginary part of the impedance should obey the mathematical constraints:[54,55]

$$Z'(\omega) = Z'(\infty) + \frac{2}{\pi}\int_0^{\infty} \frac{xZ''(x) - \omega Z''(\omega)}{x^2 - \omega^2} dx \qquad \text{(Equation 13)}$$

$$Z''(\omega) = -\frac{2\omega}{\pi}\int_0^{\infty} \frac{Z'(x) - \omega Z'(\omega)}{x^2 - \omega^2} dx \qquad \text{(Equation 14)}$$

Where $Z'(\omega)$ and $Z''(\omega)$ represent the real and the imaginary part of the impedance, respectively.

The modeling function can be determined by relative residuals of the real part $\Delta_{Re}(\omega)$ and the imaginary part $\Delta_{Im}(\omega)$, which are defined as:[52,56,57]

$$\Delta_{Re}(\omega) = \frac{Z'(\omega) - \widehat{Z}'(\omega)}{|\widehat{Z}(\omega)|} \qquad \text{(Equation 15)}$$

$$\Delta_{Im}(\omega) = \frac{Z''(\omega) - \widehat{Z}''(\omega)}{|\widehat{Z}(\omega)|} \qquad \text{(Equation 16)}$$

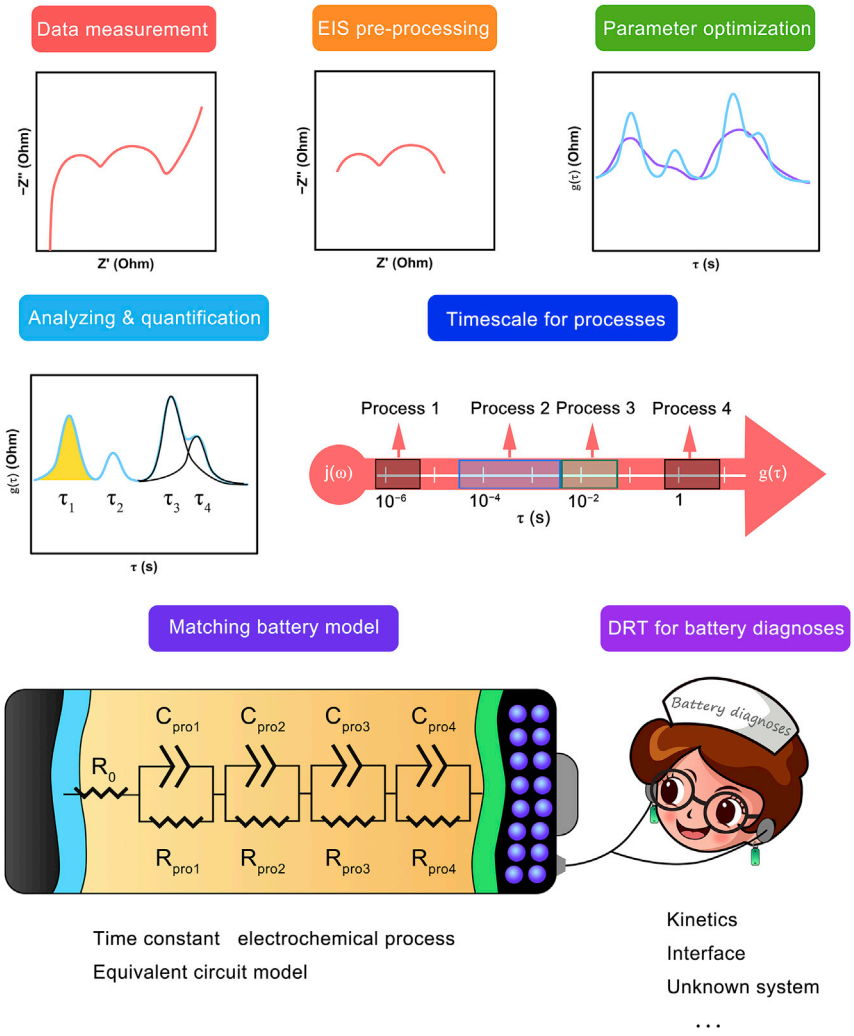

Figure 2. Workflow for DRT-based timescale diagnoses for the battery system

Where $Z(\omega)$ represents the impedance measured at frequency ω and the $\hat{Z}(\omega)$ represents the modeling impedance at frequency ω (ω=2πf, f represents the frequency.). $|\hat{Z}(\omega)|$ means the absolute value of modeling impedance. If the relative residual is lower than 1%, the impedance dataset can be validated, satisfying the Kramers-Kronig relation.[37,52] The Kramers-Kronig test is always neglected in the electrochemistry area. Only the impedance datasets that satisfied the Kramers-Kronig relation can be analyzed subsequently. In the practical application view, the EIS quality can be scored by the algorithm developed by Liu et al. according to the Bayesian Hilbert transform (BHT) method.[53] Schönleber et al. developed the open-access "Lin-KK" tool for the Kramers-Kronig validity test.[58]

The acquired EIS results should be pre-processed. Considering conventional DRT solution, the divergent EIS, such as capacitive diffusion branch characteristic and the inductance, should be subtracted before DRT transition.[59] The pre-processed EIS will be transited into DRT plots by specific algorithms. The peaks can be directly identified presenting the specific electrochemical processes. Virtually, the pre-processing for capacitive

Please cite this article in press as: Lu et al., The timescale identification decoupling complicated kinetic processes in lithium batteries, Joule (2022), https://doi.org/10.1016/j.joule.2022.05.005

diffusion can be omitted with advanced algorithms such as generalized distribution of relaxation time (GDRT) or coupling with the DDC and DDT methods.[47,60]

Optimizing parameters for DRT

The parameters for DRT calculation are of great significance. The solution toward $g(\tau)$ is an "ill-posed problem," which means that the possible solution is not unique.[26] This is an intrinsic mathematic problem. The regularization parameter and the full width at half maximum (FWHM) are common pre-set parameters for the DRT algorithm according to the Tikhonov regularization.[15] It is proved that the selection of different parameters will significantly influence the DRT results. There are some methods to optimize the parameters. The parameter optimization is crucial to achieving accurate DRT results and is also greatly developed. Ciucci's group put forward the real and imaginary cross-validation test functions to select the regularization parameter and compared the ridge regularization and the least absolute shrinkage and selection operator (Lasso) regularization.[61] The Lasso regression should be conducted accompanied by the ridge regularization.[61] The L-curve method can also be used to optimize the regularization parameter in the ridge regularization process.[62] Li et al. utilized the Elastic net regularization, which combines the advantage of the ridge and Lasso regularization simultaneously with automatic optimal tuning parameter by the information criteria.[28] This method can realize accurate estimating of EIS data and suppress the pseudo peaks in DRT. Hahn et al. compared the optimized regularization parameter with the discrepancy, cross-validation, and L-curve optimum criteria.[37] The repetitive impedance measurement methods combined with statistical resampling can search the optimal regularization parameters.[63] The comparative measurements under the same circumstances help to distinguish the statistical noise. Schlüter et al. also developed this method to access the optimal regularization parameter from only one EIS result avoiding the repetitive measurements.[36] The reverse transformation as "DRT to EIS" is also effective to verify the accuracy and consistency of the DRT compared with the original EIS.[64] In addition, some developed algorithms can avoid adjusting parameters for DRT transition by optimizing the Tikhonov regularization methods.[38]

Analyzing and quantification

The most important step for DRT is to identify the specific electrochemical processes through the time constants, which requires a picture of physical or chemical meanings in battery systems. Briefly, the timescale for basic electrochemistry processes is unraveled. At once, the DRT plots are acquired, and the independent time constant peaks can be directly ensured. The coupled peaks may occur sometimes, which can be separated by multi-peaks resolution methods and conduct the subsequent impedance quantification.

Interpreting electrochemistry processes in the timescale

The timescale peaks are distinguished through the DRT methods, representing the time constant of different electrochemical processes. Consequently, determining the physical meaning of different time constants is the core issue for DRT analysis. Many electrochemical processes still remain unresolved for some novel battery systems, which are the target for subsequent diagnoses.

Battery modeling and diagnosis

Constructing the relationship between timescale parameters with their real electrochemical processes helps to build the real timescale-based battery model. It is easy to identify the different electrochemical processes in timescale and quantify their

Please cite this article in press as: Lu et al., The timescale identification decoupling complicated kinetic processes in lithium batteries, Joule (2022), https://doi.org/10.1016/j.joule.2022.05.005

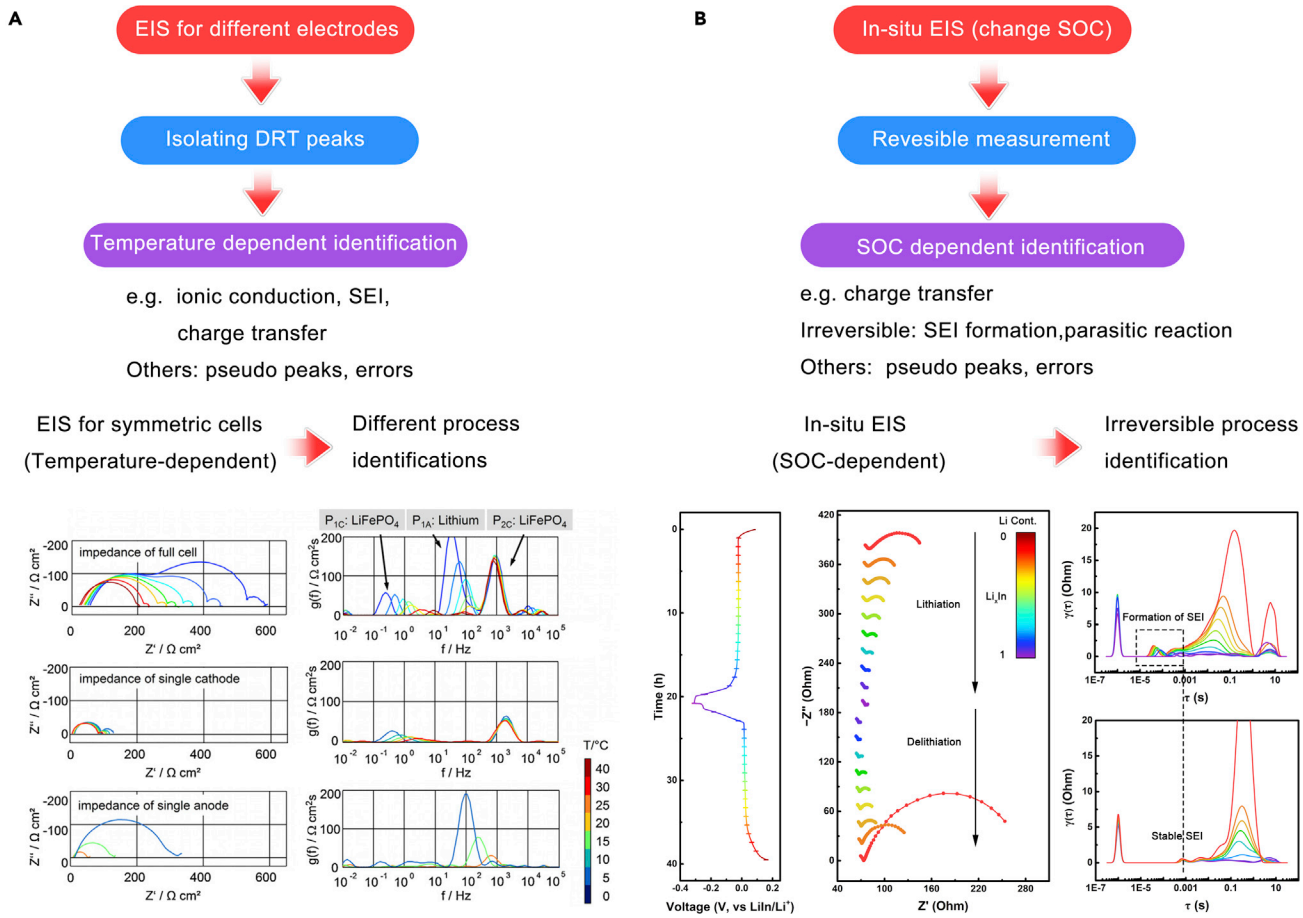

Figure 3. The DRT peak identification by temperature-dependent route[59] and SOC-dependent route[65]
Reproduced with permission.[59] Copyright 2011, Elsevier.

evolutions by the DRT methods. Analyzing unknown battery systems, monitoring internal evolution, optimizing the ECM model, etc. can be realized.

Timescale property

Method to identify the timescale characteristics

Ensuring the timescale-based real processes is the core issue in DRT analysis. On one hand, the timescale is identified by related theory and experimental results. On the other hand, identification of the physical meaning of a specific time constant requires the experimental design. After using appropriate parameters or algorithms, the pseudo peaks can be suppressed. Then the peak identifications can be realized in the following workflows (Figure 3).

Separating the electrochemical process

In the battery configuration view, the electrochemical processes mainly include electrolyte-based responses, anodic responses, cathodic responses, and accessories-based responses such as particle contact and current collector interfaces. In the Li kinetics view, the electrochemical processes include the ionic conduction process, interfacial formation process, charge transfer process, side reaction process, bulk diffusion in materials, etc. Fundamentally, measuring symmetric cells assembled

Please cite this article in press as: Lu et al., The timescale identification decoupling complicated kinetic processes in lithium batteries, Joule (2022), https://doi.org/10.1016/j.joule.2022.05.005

with only anodes or cathodes is mainly is basic to isolate the anodic-, cathodic-, and electrolyte-based responses in the battery configuration view.

For instance, Schmidt et al. separated the kinetics in Li/$LiFePO_4$ batteries by measuring different symmetric cells of Li/Li and $LiFePO_4$/$LiFePO_4$.[59] Then the kinetics process of Li and $LiFePO_4$ are distinguished from the full cells (Figure 3A). The identification of the anodic, catholic, and electrolyte responses by symmetric cells has also been utilized in many DRT analyses.[66–68]

Identify the static/dynamic and reversible process

However, the anodic or cathodic processes also possess static and dynamic processes. The dynamic processes mean the electrochemistry process that can be influenced by the state of the charge. In contrast, the static processes remain stable during charging or discharging. For instance, the interfacial charge transfer is a typical dynamic process, which is influenced by the phase composition, ionic concentration, etc. The ionic conduction in solid-electrolyte interphase (SEI) is a typical static process. The electrolyte responses are also static processes and mainly exist in solid-state batteries, which can be easily identified.[69]

The SOC-dependent process can help to distinguish between the dynamic and the static process. Hence, the half-cell is widely used in SOC-dependent analyses. Reversibility is one of the most important criteria to identify different processes. The charge transfer processes exhibit strong reversibility. The lithium concentration in the electrodes or interfaces influences the exchange current density, resulting in the continuous changes of charge transfer impedance.[65,70] The SEI formation and the parasitic reaction are not reversible. The ionic condition and the accessory-based process are SOC-independence exhibiting static features. The SOC-dependent identifications require *in situ* EIS or GEIS measurement in reversible cycles to guarantee accuracy. For instance, Lu et al. used the solid-state half-cell, separating the SEI formation processes by changing the SOC during the cycling of Li-In alloy.[65] During the lithiation and delithiation process, the irreversible SEI formation and reversible charge transfer process can be clearly identified (Figure 3B). The SOC-dependent methods in half-cells can realize the analyses of single electrode behaviors. The SEI formation and charge transfer evolution in graphite anode are unraveled by DRT cooperating with GEIS regulated SOC.[18] If the half-cell is measured in three electrodes with a reference electrode, the accuracy will be further improved. The SOC-dependent method can clearly distinguish the basic reversible processes, define the physical meanings of the reversible peaks, and find the irreversible formation processes.

Temperature-dependent analyses

The electrochemistry processes are commonly temperature dependent. Considering the activation energy (E_a), the relationship is described as[18]:

$$R_x = R_0 e^{\frac{E_a}{RT}} \quad \text{(Equation 17)}$$

The different E_a of each electrochemistry process is the fingerprint to identify the processes, which is the key issue for the time constant identification.

As evaluated in graphite-NCM 18650 batteries, the E_a of charge transfer, SEI/cathodic electrolyte interphase (CEI), and contact impedance reach 60, 48, and 25 kJ mol^{-1}, respectively.[71] Zhou et al. also provided the activation energy in 24 Ah NCM111-graphite pouch cells as 0.09 eV for contact, 0.16 eV for Ohm resistance, 0.79 eV for SEI, and 0.67 eV for charge transfer on the cathode.[72] The

Please cite this article in press as: Lu et al., The timescale identification decoupling complicated kinetic processes in lithium batteries, Joule (2022), https://doi.org/10.1016/j.joule.2022.05.005

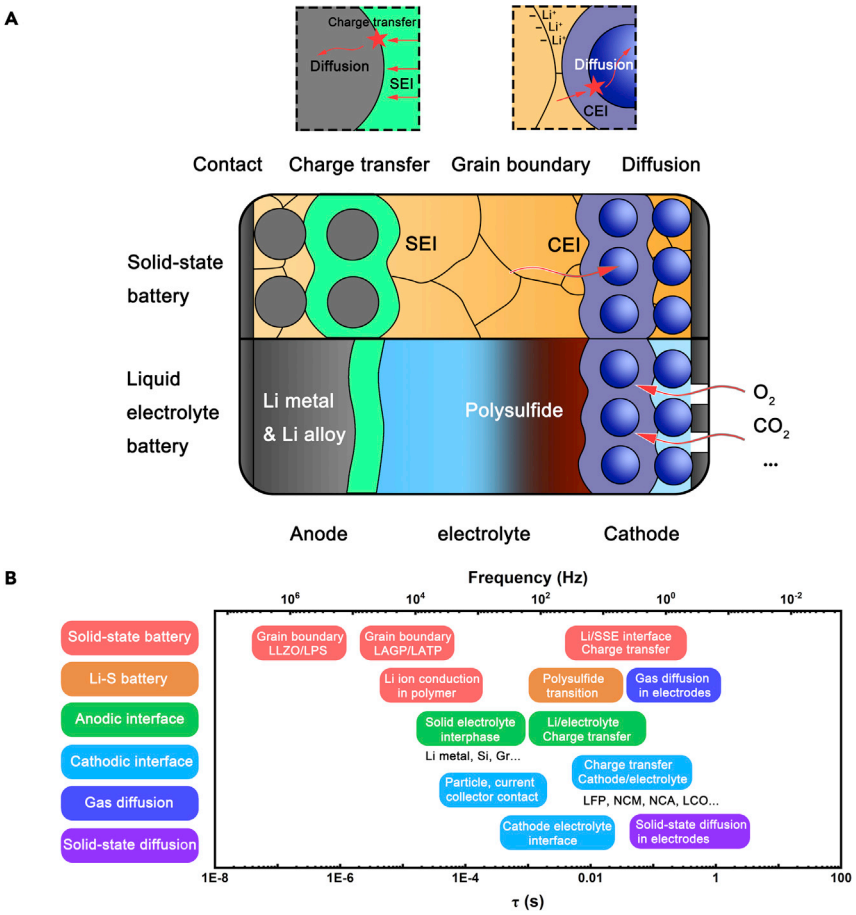

Figure 4. Typical kinetics processes and related time constant in various batteries

(A) Typical kinetics processes in the battery.

(B) The time constant of different kinetic processes.

charge transfer of Li metal reaches 0.47 eV.[59] Utilizing the temperature-dependent method can direct connect the physical properties of different electrochemical processes. Confronting complex electrochemistry systems, such as systems with multiple reversible and dynamic processes, the temperature-dependent method is more effective.

Looking up the timescale dictionaries

The time constants in battery systems have been gradually accumulated by DRT-based timescale analyses. With the enrichment of timescale dictionaries, the EIS interpreted by DRT can be accomplished rapidly. The timescale datasets are introduced subsequently.

The time constant for typical electrochemical processes

The basic processes in batteries mainly include conduction-based process, charge transfer-based process, physical contact, and diffusion processes, which are also unique in their specific systems (Figure 4A). Basically, the conduction-based process is much faster, relating to quick relaxation. Considering the $\tau = RC$, the differences in time constant can be clearly understood. The quick conduction will lead to low concentration differences, leading to low capacitance. Hence, the conduction-based processes commonly possess very small relaxation time such as grain

Please cite this article in press as: Lu et al., The timescale identification decoupling complicated kinetic processes in lithium batteries, Joule (2022), https://doi.org/10.1016/j.joule.2022.05.005

boundary conduction of 10^{-7} to 10^{-5} in different solid-state electrolytes. Virtually, the ionic transport in the grain boundary of different SSEs also possesses discrepancies. The relaxation time of the ionic transport across grain boundary in $Li_7La_3Zr_2O_{12}$ (LLZO) and some sulfide solid-state electrolytes are at the level of 10^{-7} to 10^{-6} s.[73–75] Different dopants will influence the time constant. The ionic transport in the grain boundary of NASICON and LLTO is different from that in LLZO or sulfide ones.[76,77] The relaxation time of grain boundary conduction directly reflects the ability of ionic conduction at the grain boundary. The impedance of SEI and CEI are both conductive films, with a time constant of 10^{-4} to 10^{-2} s, which is related to the conductivity. Typically, the time constant of SEI in solid-state batteries ranges from 10^{-4} to 10^{-3} s.[78,79] The time constants of graphite SEI range from 10^{-3} to 10^{-2} s measured with EC/DEC electrolytes.[17,18] The time constant of SEI and CEI may exist at the same orders of magnitude in different works. In the same battery system, a three-electrode or half-cell system can help to clearly distinguish them. The charge transfer in batteries mainly represents interfacial electrode reactions, which are sluggish processes.[79] Comprehensively, the charge transfer at the Li/electrolyte interface is more rapid than that of cathode materials delivering the time constant of 10^{-2} to 10^{-1} s, which is consistent with that in a solid-state system. Sulfur is a special cathode material delivering a series of redox processes during the lithiation. The kinetics of the lithiation toward sulfur cathode is highly related to the solubility of the formed polysulfide. The solid-liquid transition (Li_2S_8–Li_2S_4) is much more rapid than the liquid-solid (Li_2S_4–Li_2S_2) and solid-solid transition (Li_2S_2–Li_2S).[80,81] The corresponding time constants range from 10^{-2} to 1 s due to the different lithiation stages. As summarized, the charge transfer of layer oxide cathode ranges from 0.4 to 40 Hz. Typical specific frequencies are 6.2–28.8 Hz for $LiCoO_2$,[82] 0.4–3 Hz for NCA,[83] and 2–14 Hz for NCM.[84] The related time constant can be calculated by $\tau = \frac{1}{2\pi f}$. These values only provide the reference for orders of magnitude due to the discrepancies in materials and measurement details. The diffusion in electrodes or materials is the most sluggish process because the diffusion is only driven by the concentration. The time constant for diffusion reaches more than 10 s every 100 s, which is the possible rate-determining step for battery kinetics. It also happens in gas electrodes in Li-O_2 batteries, fuel cells, and ionic diffusion in intercalation materials.[85] Virtually, the intrinsic concentration also reflects the relaxation time. It is reported that a higher concentration of lithium in negative electrodes and a lower concentration in positive electrodes will result in prolonged relaxation time.[13] Hence, the typical time constant of specific processes always exhibits a range but not an accurate value. The total timescale distributions of different kinetics processes are summarized in Figure 4B, and the related data are displayed in Table 1.

POTENTIAL APPLICATIONS FOR TIMESCALE DIAGNOSIS

Constructing an electrochemistry model

Rationally interpreting EIS requires constructing an accurate electrochemistry model. The DRT method can distinguish the kinetics process, avoiding extremely subjective judgment. The DRT method helps to deepen the electrochemistry understating in special battery systems such as Li-S batteries. The continuous evolution of soluble polysulfide with different sulfur chains will change the electrochemistry properties.[94,95] The peculiar solution-deposition mechanism will also result in different electrochemistry properties compared with conventional cathodes. The polysulfide electrochemistry can be analyzed by in timescale view. Risse et al. analyzed the time constant and related impedance of polysulfide (Li_2S_x, $2 < x < 8$; Figure 5).[80] The specific charge transfer time constants of polysulfide range from

Please cite this article in press as: Lu et al., The timescale identification decoupling complicated kinetic processes in lithium batteries, Joule (2022), https://doi.org/10.1016/j.joule.2022.05.005

Table 1. The kinetics processes in different batteries and their related time constants or specific frequencies

Kinetics process	Time constant (s)	Specific frequency $\left(\tau = \frac{1}{2\pi f}\right)$, Hz	Battery system	Methods	Algorithm	References
Grain boundary of solid-state electrolyte						
Al-doped LLZO	10^{-6} s	159 kHz	Symmetric cell	EIS, DRT	DRTtools	75
Ta-doped LLZO	$<1.6 \times 10^{-7}$ s	>1 MHz	Symmetric cell	EIS	–	73,74
Ga-doped LLZO	3.2×10^{-7} s	500 kHz	Symmetric cell	EIS, DRT	ED-DRT	86
Nb-doped LLZO	$<1.6 \times 10^{-7}$ s	>1 MHz	Symmetric cell	EIS	–	74
LAGP	$\sim 7.5 \times 10^{-7}$ s (273 K)	~210 kHz (273 K)	Symmetric cell	EIS	–	87
$Li_7P_3S_{11}$	2.5×10^{-6} s (273 K), > 1.6×10^{-7} s (298 K)	63 kHz (273 K), >1 MHz (298 K)	Symmetric cell	EIS	–	88
Li_6PS_5Cl	$<1.6 \times 10^{-7}$ s	>1 MHz	Symmetric cell	EIS	–	89
Polymer ionic conduction						
PEO	10^{-5} s (298 K)	15.9 kHz	Symmetric cell	EIS, DRT	EC-idea	29
SEI & CEI						
SEI of Li-graphite	10^{-3} to 10^{-2} s	160–16 Hz	Half-cell	Three electrodes, GEIS, DRT	LMA	18
SEI of Li-graphite	1.6×10^{-4} s	500 Hz	3.3 Ah full cell	EIS, DRT	EC-idea	90
SEI of Li-Si	1.6×10^{-4} to 1.6×10^{-3} s	10^4–10^3 Hz	Half-cell	EIS, DRT	DRTtools	79
SEI of Li metal	1.6×10^{-2} s	10^2 Hz	Symmetric cell/ full battery	EIS, DRT	–	59
SEI of K–graphite	10^{-3} to 10^{-2} s	160–16 Hz	Half-cell	EIS, DRT	DRTtools	17
SLEI of LiPON/DME	10^{-3} s	160 Hz	Symmetric cell	EIS, DRT	DRTtools	78
CEI of NCM	$3.7–6.7 \times 10^{-3}$ s	43–24 Hz	20 Ah full cell	GEIS, DRT	DRTtools	84
CEI of NCA	1.6×10^{-4} to 1.6×10^{-3} s	1000–100 Hz	3.2 Ah 18,650 full cell	GEIS, DRT	DRTtools	83
Charge transfer						
Li-graphite	10^{-2} to 10^{-1} s	16–1.6 Hz	Half-cell	EIS, DRT	LMA	18,71
Li-graphite	0.016 s	10 Hz	3.3 Ah full cell	EIS, DRT	EC-idea	90
Li-graphite	0.01 s	15 Hz	Half-cell	GEIS, DRT	DRTtools	66
Li-graphite	3.2×10^{-3} s	50 Hz	3.3 Ah pouch cell	GEIS, DRT	DRTtools	66
Li-Si	1.6×10^{-3}–1.6 s	10^2–0.1 Hz	Half-cell	EIS, DRT	DRTtools	79
Li_xIn ($0 < x < 1$) Li_xIn ($1 < x < 1.25$) Li_xIn ($1.25 < x < 1.5$)	10^{-3} to 10^{-2} s 10^{-1} s 10^0 to 10^1 s	160–16 Hz 1.6 Hz 0.16–0.016 Hz	Symmetric cell	GEIS, DRT	DRTtools	65
Li metal	1.6×10^{-3} to 1.6×10^{-2} s	10^2–10 Hz	Symmetric cell/ full cell	EIS, DRT	–	59
Li metal	1.6×10^{-3} s	10^2 Hz	Symmetric cell	EIS, DRT	DRTtools	66
Li metal/LLZO	~0.11 s	~1.4 Hz	Symmetric cell	EIS, DRT	–	91
K–graphite	10^{-2} to 1 s	16–0.16 Hz	Half-cell	EIS, DRT	DRTtools	17
$LiCoO_2$	5.5×10^{-3}–2.6×10^{-2} s	28.8–6.2 Hz	Full cell, three electrodes	Three-electrode, GEIS	–	82
$LiCoO_2$	0.2–0.05 s	8–3 Hz	3.3 Ah pouch cell	GEIS, DRT	DRTtools	66
NCM	10^{-1}, 1.1×10^{-2} to 8.0×10^{-2} s	1.6 Hz, 14–2 Hz	20 Ah full cell	GEIS, DRT	DRTtools	22,71
NCA	0.053–0.398 s	3–0.4 Hz	3.2 Ah 18,650 full cell	GEIS, DRT	DRTtools	83
$LiFePO_4$	1.6–0.16 s	10–1 Hz	Symmetric cell/ full battery	EIS, DRT	–	59
Polysulfide	$\sim 10^{-3}$ s	~160 Hz	Symmetric cell/ full cell	EIS, DRT	LMA	80
Polysulfide	0.3×10^{-3}–50×10^{-3} s	531–3.18 Hz	Full cell	EIS, DRT	DRTtools	92
Diffusion						
O_2 in Li-O_2	>0.016 s	< 10 Hz	Full cell	EIS, DRT	DRTtools	85
Polysulfide diffusion	0.4 s	0.4 Hz	Full Li-S cell	EIS, DRT	DRTtools	92
Li^+ in Si	10–10^2 s	0.016–1.6×10^{-3} Hz	Half-cell	EIS, DRT	DRTtools	19

(*Continued on next page*)

Please cite this article in press as: Lu et al., The timescale identification decoupling complicated kinetic processes in lithium batteries, Joule (2022), https://doi.org/10.1016/j.joule.2022.05.005

Table 1. *Continued*

Kinetics process	Time constant (s)	Specific frequency $\left(\tau = \frac{1}{2\pi f}\right)$, Hz	Battery system	Methods	Algorithm	References
Other kinetics						
$Li_7P_3S_{11}$-In block electrode interface	10^{-5} s	15.9 kHz	Symmetric cell	EIS, DRT	DRTtools	65
Current collector	1.6×10^{-6} s	100 kHz	3.2 Ah 18,650 Full cell	EIS, DRT	DRTtools	83
Internal particle contact	3×10^{-6} s	53 kHz	Full Li-S cell	EIS, DRT	DRTtools	92

The experimental details such as battery configuration and the used algorithm are also summarized for comparison.
Notes: DRTtools is the DRT toolbox developed by Professor Ciucci's group.[26] EC-idea is the DRT toolbox developed by Professor Danzer's group.[37,60] LMA means the Levenberg-Marquardt algorithm. ED-DRT is the DRT solution developed by Professor Clematis's team.[93] GEIS means the galvanostatic electrochemical impedance spectra.

$\sim 10^{-2}$ to 1 s. The S_8 and Li_2S exhibit integral high kinetic impedance. Song et al. subsequently study the electrochemistry feature of the porous sulfur cathode. They utilized DRT to ensure the different processes of 10^5 to 10^3 Hz as particle contact, polysulfide evolution (Li_2S_6) at 10–1 Hz, and the diffusion <1 Hz.[67] The impedance in Li-S batteries is not only contributed by the Li-polysulfides. The Li-S full battery is also studied in different SOC statuses to identify and quantify other processes. In working Li-S batteries, Soni et al. utilize the DRT to ensure the dynamic processes that contribute to the total polarizations.[92] The Li-S full batteries possess 8 physical processes of inter-particle contact, double layer capacitance, SEI, three positive electrode charge transfer, and the diffusion for polysulfide and Li-ion. The direct research by DRT in full batteries proves that DRT helps to bridge each timescale property in full batteries with the battery status, which not only nourishes the mechanism studies but also can fulfill practical applications.

The DRT method can demonstrate the electrochemistry feature of polysulfide, including the time constant and the related impedance, and also helps to build the electrochemistry models of the Li-S battery and the porous sulfur cathode. The DRT method is also promising to unravel some hidden kinetics phenomena in novel electrochemistry systems such as Mg/Zn/Al-S or Li/Na/Zn-air/CO2 batteries and the related solid-state batteries, etc.[96]

Interfacial mechanism study

The interfacial evolution including the SEI, CEI formation, charge transfer evolutions, solid-liquid interphase formation in hybrid batteries, and solid-solid interface identifications all exhibit distinct properties. The timescale-based analyses can exhibit the formation process much more clearly than the EIS plots by DRT methods. The evolutions are always cooperating with the comparison among a series of EIS methods.

The formation of SEI on graphite anodes is detected by EIS and analyzed by the DRT. Clear SEI response can be detected at τ of 10^{-3} to 10^{-2} s.[18] The charge transfer evolution of anode and cathode during different SOC stages can also realize a timescale evaluation in different half cells[18] and three-electrode mode,[97] respectively. The anodic evolution of charge transfer is located at 10^0 Hz and the cathode charge transfer exhibit an evolution range from 10^{-1} to 10^1 Hz. The Li SEI formation can also be identified at 10^3 Hz.[84] The timescale-based analyses clearly displayed the SOC-induced evolution in full batteries. The solid-liquid interface is another kind of SEI in essence. The continuous standing impedance can be displayed clearly in

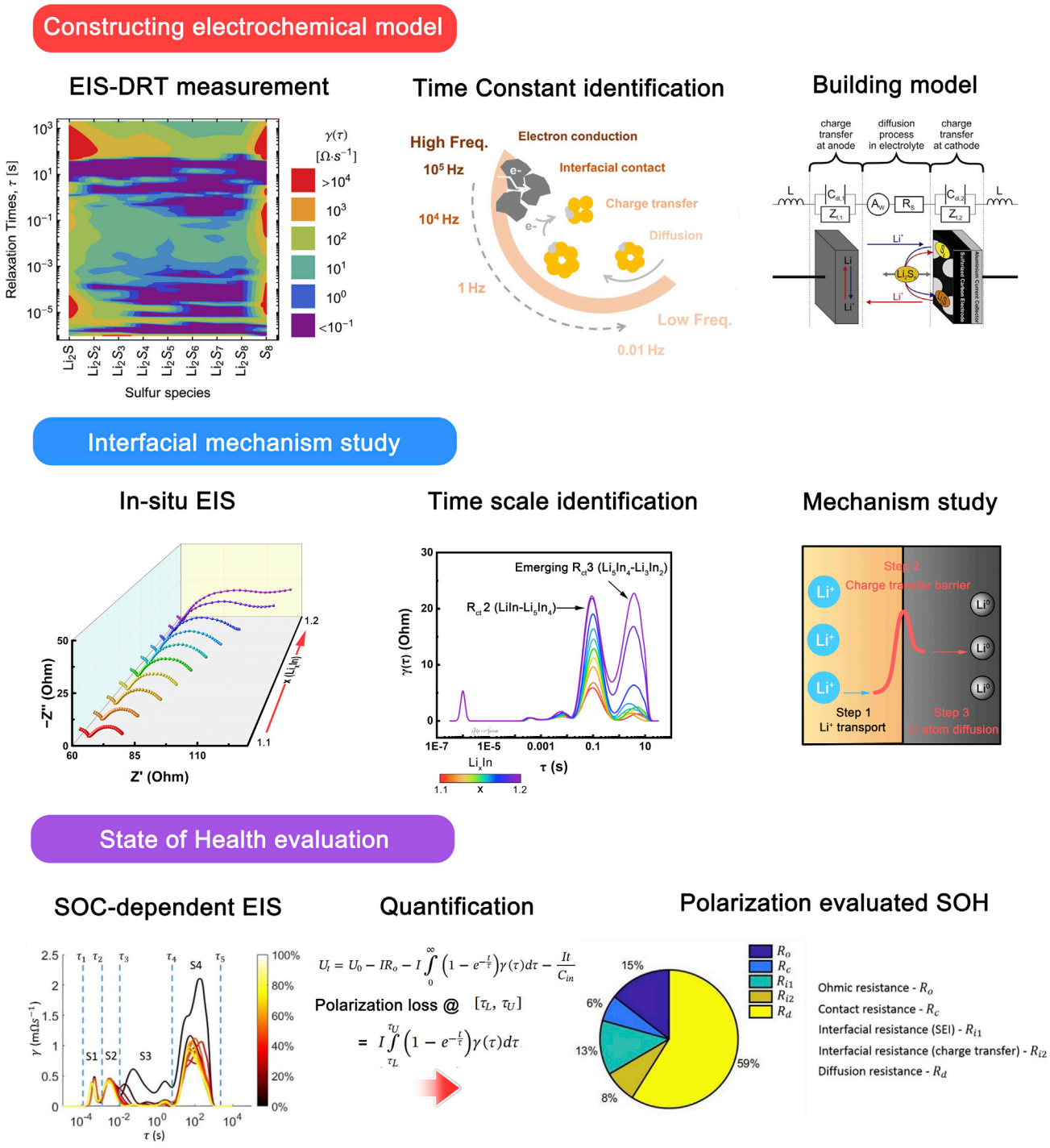

Figure 5. Applications of DRT on constructing electrochemistry model (Li-S batteries),[67,80] interfacial studies (Li-In alloy in solid-state batteries),[65] and SOH evaluation[72] according to the polarization loss quantified by DRT

Reproduced with permission.[80] Copyright 2016, Elsevier. Reproduced with permission.[72] Copyright 2019, Elsevier.

the timescale. A changed peak at τ of 10^{-3} s can be distinguished, which represents the solid-liquid interface (SLEI). Solid-state batteries are still emerging new battery systems. The related ECM is still imperfect to demonstrate the real situations.

Please cite this article in press as: Lu et al., The timescale identification decoupling complicated kinetic processes in lithium batteries, Joule (2022), https://doi.org/10.1016/j.joule.2022.05.005

Some of the timescale-based properties are still elusive.[98] Timescale identification by the DRT will provide high resolution on basic EIS interpretation. The solid-solid interface will deliver an obvious ionic capacitance behavior.[99] The ionic conduction at the grain boundary, the bulk, and the contact interfaces can be identified in timescale, respectively.[86] The ECM can be constructed according to the mentioned results. Cooperating with GEIS, the interfacial evolution can be clearly displayed. As displayed in Figure 5 (middle figure), after the evaluation of *in situ* EIS, the charge transfer evolution induced by phase transitions from LiIn, Li_5In_4, to Li_3In_2 are clearly shown in the timescale.[65] Then, the kinetics model during lithiation of alloy anode in solid-state batteries can be constructed after clearly understanding the charge transfer and diffusion processes.

State of health (SOH) evaluation

State of health is defined as the general conditions of batteries compared with a fresh one, which is highly related to some specific kinetic parameters. The complex battery kinetics will influence each other and the key issues for battery aging are hard to decouple. The timescale analyses can clearly distribute and monitor the specific kinetics during the aging processes, which help to ensure and quantify specific rate-determining steps. The operando measurement and timescale analyses play vital roles to build the model toward SOH estimations. By applying GEIS and DRT, Sabet et al. ensured the predominant process in graphite-NCA commercial batteries in different SOC, which extracts the SEI and charge transfer-based kinetics as key processes to provide parameters for evaluating SOH.[83] The calendric aging will lead to the evolution of time constants of SEI or charge transfer-based processes. Their changing tendency can also be further demonstrated by $\tau_x = R_xC_x$. For instance, the decreased τ_{SEI} during calendric aging is always attributed to the SEI growth delivering lower capacitance (C_x). The increased τ_{NMC} during cycling can be attributed to the increased $C_{charge\ transfer}$, which is directly related to the particle cracking of active materials.[22] Polarization growth means battery aging. Hence, the DRT can help to quantify the polarization loss induced by different kinetic processes, which is also important to assess the SOH.[72] The quantification of polarization loss is calculated as following[72]

$$U_t = U_0 - IR_0 - I\int_0^{\infty}\left(1 - e^{-\frac{t}{\tau}}\right)\gamma(\tau)d\tau - \frac{It}{C_{in}} \quad \text{(Equation 18)}$$

Where U_t and U_0 mean the terminal voltage and initial open-circuit voltage of the battery at the adopting current of I. C_{in} means the internal capacity.

The polarization loss (U_L) of impedance at time constant ranging $[\tau_1, \tau_2]$ is written as[72]

$$U_L = I\int_{\tau_1}^{\tau_2}\left(1 - e^{-\frac{t}{\tau}}\right)\gamma(\tau)d\tau \quad \text{(Equation 19)}$$

Hence, DRT results have been utilized to calculate the polarization loss, and the polarization loss of different kinetic processes can also be achieved. Briefly, the timescale analyses can rapidly extract key parameters for operated batteries, which are essential to provide information for modeling SOH evaluation systems.

Available solutions for DRT

Solution tools on the MATLAB platform

"DRTtools" is the online open-access tool for DRT analyses, which is developed by Professor Francesco Ciucci's team from Hong Kong University of Science and Technology.[26] This powerful tool is based on the MATLAB GUI toolbox, which has been widely applied

Please cite this article in press as: Lu et al., The timescale identification decoupling complicated kinetic processes in lithium batteries, Joule (2022), https://doi.org/10.1016/j.joule.2022.05.005

in many publications on electrochemistry studies.[19,20,26,65,72,75,83–86,100–102] The codes are provided at https://github.com/ciuccislab/DRTtools/.

"EC-Idea" tool based on the MATLAB platform is another powerful solution for comprehensive EIS study including realizing the pre-test of the Kramers-Kronig validity test, equivalent circuit fitting, and the DRT analysis. This tool was developed by Professor Michael Danzer's team from The University of Bayreuth, which has been successfully used in these publications.[29,37,60,103] The codes are provided at https://www.ees.uni-bayreuth.de/en/ec-idea/index.html.

"EIS DRT" tool developed by Xin Li and Sergei V. Kalinin's team from Oak Ridge National Laboratory is provided free online.[28] The codes are provided at https://github.com/nonmin/EIS-DRT.

Solutions in Python

Professor Ciucci's team have provided a series of contributions based on Python as:

"GP-DRT," with Gaussian process and machine learning,[34] "fGP-DRT," based on the finite Gaussian process,[41] "DP-DRT," which is called the deep prior DRT,[104] "BHT," according to the Bayesian Hilbert transform method,[53] and "GP-HT," based on the Gaussian process Hilbert transform method.[55] All the codes and tutorials are applied online at https://github.com/ciuccislab.

Professor Andrei Kulikovsky from the Institute of Energy and Climate Research developed the Tikhonov regularization with the projected gradient iterations (TRPG) method for the DRT and provided the open-access Python code.[105] The codes are provided at https://github.com/akulikovsky/DRT-python-code.

Independently developed software

"ISGP," called impedance spectroscopy genetic programming, is a DRT solution from the genetic programming method developed by Professor Yoed Tsur's team from the Israel Institute of Technology.[35,40,106]

"DFRT-Py" is developed by Mark Žic et al. from the Johann Radon Institute for Computational and Applied Mathematics.[107,108]

"ED-DRT" is developed by Professor Davide Clematis et al. from the University of Genoa, with the open-access share.[93]

"RelaxIS" with the DRT function module developed by the Metrohm. Corp. can realize the in-time DRT analyses for EIS data acquired on the Metrohm. electrochemistry station.

The "Lin-KK" tool is developed by Professor Schönleber et al. from Karlsruhe Institute of Technology (KIT). This tool is used for the EIS Kramers-Kronig validity test.[58]

EMERGING APPLICATIONS FOR TIMESCALE ANALYSES

The DRT-based timescale analyses possess the potential for practical applications. The timescale analyses are the non-destructive methods, which is one of the most priority for battery monitoring. EIS measurement and DRT transition are all time-saving measurements that can be accomplished in only several minutes. DRT is also a data mining tool for EIS results, which is beneficial to provide more information and build datasets.

Please cite this article in press as: Lu et al., The timescale identification decoupling complicated kinetic processes in lithium batteries, Joule (2022), https://doi.org/10.1016/j.joule.2022.05.005

From 1D-DRT to multidimensional-DRT

It is discussed that conventional DRT is limited by the data accuracy and the hyperparameter for regularization. One of the major reasons is that the EIS is only interpreted as a function of frequency (1D data, only relative to frequency). Hence, the DRT interpreted according to only frequency is called 1D-DRT. If the EIS spectra are measured at different external circumstances (e.g., temperature, different battery stages, other experimental conditions, etc.) forming the EIS datasets, the limitations will be loosened from only frequency to the multidimensional experimental conditions.[109] In addition, the analyses of DRT can connect the data dependency with the frequencies and the experimental conditions. The multidimensional-DRT is promising to increase accuracy and expand new application functions. Mertens et al. first put forward the 2D-DRT, importing a new dimensional of temperature, which reduces the uncertainty of EIS, contributing to the increased resolution.[110] Kim et al. expended more dimension from experimental conditions of the different gas environments during evaluating the EIS from the perovskite solar cells.[111] They conducted the multivariate analysis applying non-negative matrix factorization (NMF) to discover the tendency in the DRT related to multiple experimental conditions. When more conditions are involved, artificial intelligence including machine learning or deep learning is a powerful way to analyze the hyper-structural EIS datasets with multidimensional conditions. Quattrocchi et al. built deep neural networks (DNNs) to examine, interpret, and unravel the EIS dependency from multiple experimental conditions.[109] 2D, 3D, and 4D experimental datasets are all attempted in different electrochemistry systems of SOFC cells and perovskite solar cells, proving the robustness and universality of deep-DRT. The deep-DRT is promising for analyzing the EIS measured in complex electrochemistry systems with multiple influence factors such as various batteries, supercapacitors, etc. Hence, the multidimensional-DRT can be suggested in the batteries industry to monitor and identify the battery status, realizing the SOC estimation, echelon use batteries, etc.

The base for data-driven modeling

Timescale deconvolution (DRT) is a physical method to vectorize the EIS data with the dimension of timescale and impedance intensity (Figure 6). Batteries with different statuses (such as SOC, aging time, cycle life, residual capacity, etc.) will exhibit specific impedance characteristics. These statuses are treated as a group of ensured targets. The measured EIS will be shown as features as two dimensions of a series of timescales and the timescale-related impedance intensity. Hence, a specific battery can be described as the vector of (timescale, impedance|battery status). Many specific batteries can form a dataset, which can build an appropriate estimation model after data-driven machine learning.

Battery classification and echelon utilization

The retired battery classifications are emerging problems and contain great business prospects and research value, which can be conducted by analyzing open-circuit voltage (OCV) and discharge curves.[112] The simple results of OCV cannot reflect a real battery SOH, and the measuring discharge curve of aged batteries is also time consuming.[113] Rapid battery sorting techniques are in urgent need with the sharp growth in the number of retired batteries. The aged batteries exhibit special impedance features, which can be distinguished by the DRT. The impedance of specific kinetic processes with the special time constants should be the key to determining the battery classifications, and the vectorized timescaled impedance datasets can also be trained into models and help to classify the aged batteries in a data-driven way. Training strategies such as clustering algorithm K-means, dimension reduction principal-component analysis (PCA), support vector machine (SVM),

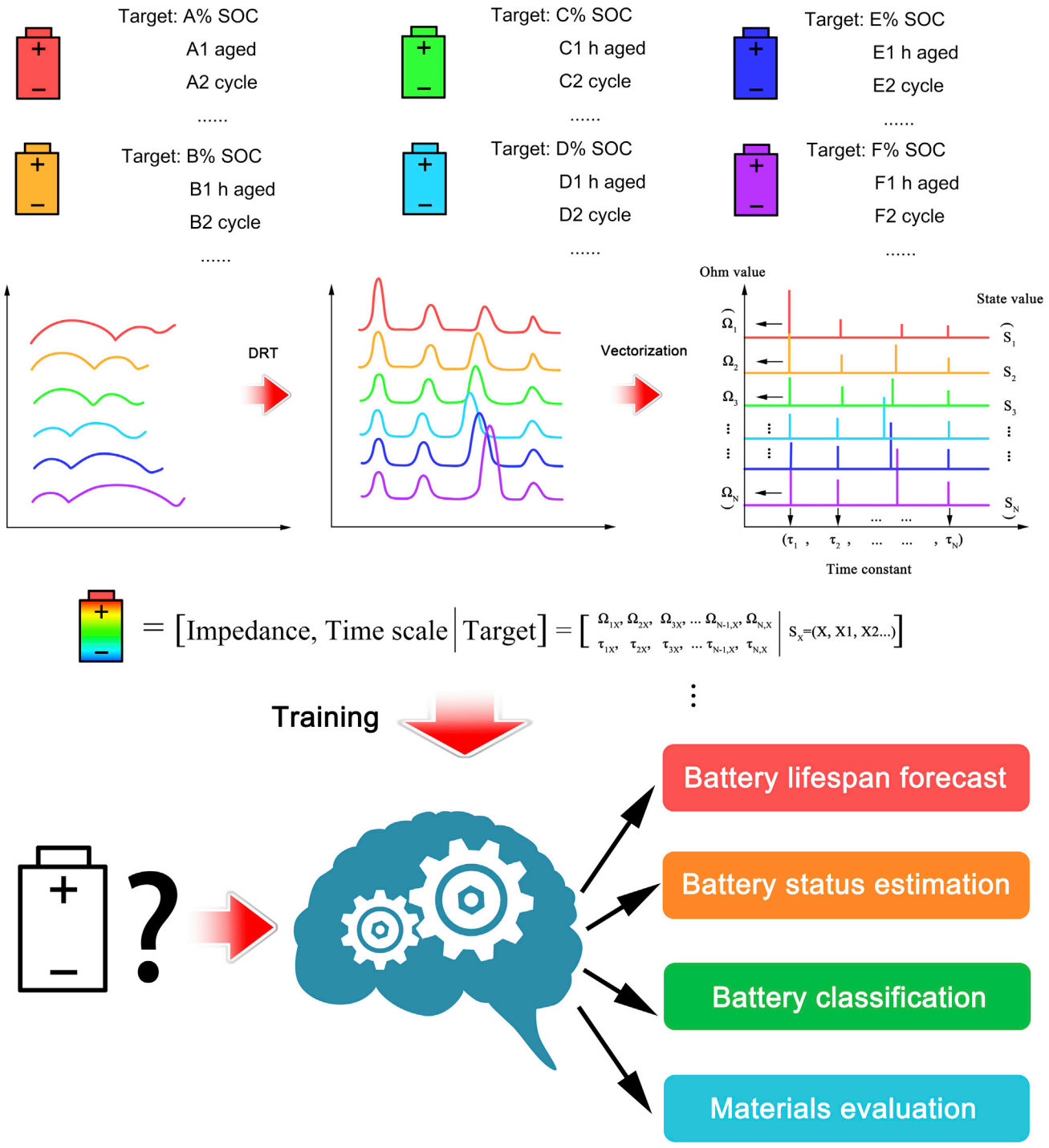

Figure 6. Battery modeling by DRT to provide the data-driven source for machine learning-based artificial intelligence (AI) prediction

random forest, etc. are all promising to realize battery classification and help to identify the key benchmark for battery sorting by using the DRT-based datasets. Compared with conventional classifications, DRT results contain more timescale information than conventional resistance, voltage, etc., which is promising to realize higher accuracy. In addition, the timescale-based retired battery classifications are promised to be accomplished in several minutes, which highly improves efficiency.

Please cite this article in press as: Lu et al., The timescale identification decoupling complicated kinetic processes in lithium batteries, Joule (2022), https://doi.org/10.1016/j.joule.2022.05.005

Lifespan estimation

The hidden information on battery lifespan can also be unraveled by EIS-based timescale analyses. The target for the battery vector can be changed as lifespan. The isolated study or data-driven study can also be conducted to build the model for battery lifespan estimation. The battery lifespan estimation is mainly related to the degradation mechanism. The degradation of batteries mainly derives from the loss of lithium-ion inventory, ohmic resistance increase, and the loss of active materials.[114] These processes are respectively related to different key kinetics processes in different timescales. The timescale-based information is also valuable to estimate the SOH of full battery and electrode status. Although the estimation should be supported by abundant historical data, the timescale-based estimation possesses adequate physical meaning, which can be highly connected with real electrochemical models.

Materials evaluations

The material features are also hidden in the timescale data. The materials transformation, SEI evolution, and other internal changes can also be reflected as impedance with the specific time constants. It will be powerful to analyze the mechanism, especially cooperating special datasets. The timescale analyses can help to estimate the contribution of different kinetics processes during different application situations such as continuous or interrupted operation, aging, environmental tolerance, etc. and can also help to distinguish material features (e.g., NCM, $LiFePO_4$, and Li-rich cathode) that provide the benchmarks and scientific support for battery optimization. Considering the battery degradation mechanism, the loss of lithium-ion inventory is highly related to the SEI growth at the anodes. The ohmic resistance increase can be attributed to the SEI growth, the decomposition of electrolytes, and material degradation. The loss of active materials is mainly ascribed to the dissolution of the cathode. The online monitoring of material kinetics is likely going to be realized in a timescale, which can provide adequate battery internal information to give early warning of risks such as Li plating, dendrite growth, electrolyte depletion, etc.[115]

Summary and perspectives

Timescale-based analyses provide opportunities to separate the coupled kinetic information in the "black box" of the batteries. It is a powerful thought to study the internal kinetics characteristics. EIS is a typical methodology to provide frequency domain-based features, which can be interpreted by DRT through isolated time constants to identify different kinetic processes. Briefly, the DRT-based timescale analyses can significantly promote the basic understandings in electrochemistry society, possessing unique advantages as follows.

Highly efficient and accurate analyses

Timescale analyses can distinguish the coupled internal electrochemical processes and monitor their evolutions during battery cycling. The DRT offers an overview and quantified characteristics of the kinetics.

Provide new insights on in timescale

Timescale analyses will contribute to exposing some hidden electrochemical processes because it does not depend on the prior understanding. Consequently, unraveling the unknown time constants will provide new insights to decouple the behaviors within the battery (e.g., kinetics interpretation).

Please cite this article in press as: Lu et al., The timescale identification decoupling complicated kinetic processes in lithium batteries, Joule (2022), https://doi.org/10.1016/j.joule.2022.05.005

Powerful reference for ECM

DRT benefits ensure the real kinetics models. They can provide additional details to modify the experienced oriented ECM, especially confronting more possible undefined models.

DRT is an efficient method that can decouple the electrochemical processes by distributing their respective timescales. New opportunities and challenges are appearing after applying the DRT concept in battery studies. From both the DRT algorithms view and their applications view, there are some potential points to develop the DRT methods and their applications in the future.

Accurate EIS measurement

The EIS accuracy is the basis for the DRT evaluation. Some measurement issues will lead to problems in EIS evaluation. The incomplete impedance data at high frequency (e.g., the incomplete semicircle of > 1 MHz for solid-state electrolyte) or the fluctuated points at low frequency will influence the results for DRT analyses.

The accuracy of the DRT algorithm

Presently, the DRT analyses still require parameter screening to realize a reliable simulation by using a specific algorithm. The regularization parameter and the FWHM will significantly influence the shape and peaks in DRT plots. In addition, the possible pseudo peaks during DRT analyses will interfere with the evaluation of electrochemistry processes, which is the major barrier for DRT applications.[116] Advanced algorithms that can automatically select parameters are essential to improving accuracy and effectivity. Developing methods to enhance the accuracy of the DRT transformation is of vital importance.

Identifying the real meaning of the specific time constant

This problem exists in evaluating a new battery system or conducting a mechanism study. Some chemical characterizations should be combined to assist the interpretation of the timescale properties such as detecting the multilayer structure, newformed interfaces, charge transfer of specific material phases, etc.

Combining DRT models with the DDT and DDC

The DDC and DDT are potential solutions to deal with the non-convergence EIS.[45–47] The DDC possesses similar thoughts that convert the EIS into complex capacitance and DDT will decouple the EIS into complex admittance. Their rational combination with DRT can realize the proper modeling of battery impedance.[45]

Expanding 1D-DRT to multidimensional-DRT

1D-DRT means that EIS is only interpreted as a function of frequency. 2D-DRT and even multiple dimensional-DRT importing the new dimensional information will reduce the uncertainty of EIS, contributing to the increased resolution. In addition, the multiple dimensional impedance data can also be deeply interpreted by multidimensional experimental conditions and the application scenarios, which can be applied in the batteries industry situations such as monitoring and identifying the battery status, realizing the SOC estimation for battery management systems, echelon use batteries, etc.

Data-driven applications for battery analyses

The timescale data can be obtained by conventional EIS even an *in situ* GEIS in different electrochemical stages. DRT methods will transform the EIS into multidimensional data delivering kinetics features and battery statuses. A series of vectors

Please cite this article in press as: Lu et al., The timescale identification decoupling complicated kinetic processes in lithium batteries, Joule (2022), https://doi.org/10.1016/j.joule.2022.05.005

can be batch produced as the dataset for estimation. Different from conventional battery datasets, the timescale datasets contain kinetics properties, which can be trained by artificial intelligence (AI) based machine learning to acquire rational physical models, building the direct connection between the status of batteries and the monitored data.

In the future, the timescale diagnoses can not only be used for academic research but also possesses practical application potential. DRT is a typical example to realize interdisciplinary between electrochemistry with the data science. After being decoupled by DRT, the battery status can be directly analyzed by multiple data methodology. The timescale data can directly point out kinetics problems and can contribute to constructing multiple models to exhibit objective laws. The battery big data era is coming with a sharp increase in battery production and applications. After adopting an advanced three-electrode test, rapid multi-sine EIS technique, etc., a huge amount of accurate timescale datasets trained by machine learning are promising to build models, which can realize the online estimation of various battery statuses such as lifespan, SOC, SOH, residual capacity, single electrode status, and safety status, in many battery application situations. The timescale diagnosis can be popularized from the lab level to industrial applications. By introducing the battery timescale diagnosis in this perspective, we hope to promote the connection between fundamental battery mechanism study and the industrial practical applications.

ACKNOWLEDGMENTS

This work was supported by the National Key Research and Development Program (2021YFB2500300), the National Natural Science Foundation of China (22109084, 22108151, and 21825501), and the China Postdoctoral Science Foundation (2019 M660659, BX20190168, and 2021TQ0164). Y. Lu and C.Z. Zhao appreciate the Shuimu Tsinghua Scholar Program of Tsinghua University.

AUTHOR CONTRIBUTIONS

Conceptualization, Q. Zhang, Y. Lu, and C.Z. Zhao; funding acquisition, Q. Zhang, Y. Lu, and C.Z. Zhao; supervision, Q. Zhang; writing – original draft, Y. Lu; writing – review & editing, C.Z. Zhao, Y. Lu, J.Q. Huang, and Q. Zhang.

DECLARATION OF INTERESTS

The authors declare no competing interests.

REFERENCES

1. Chen, R., Li, Q., Yu, X., Chen, L., and Li, H. (2020). Approaching practically accessible solid-state batteries: stability issues related to solid electrolytes and interfaces. Chem. Rev. *120*, 6820–6877.

2. Lu, Y., Zhao, C.-Z., Yuan, H., Hu, J.-K., Huang, J.-Q., and Zhang, Q. (2022). Dry electrode technology, the rising star in solid-state battery industrialization. Matter *5*, 876–898.

3. Chen, J., Wu, J., Wang, X., Zhou, A.a., and Yang, Z. (2021). Research progress and application prospect of solid-state electrolytes in commercial lithium-ion power batteries. Energy Storage Mater. *35*, 70–87.

4. Li, Y., and Guo, S. (2021). Material design and structure optimization for rechargeable lithium-sulfur batteries. Matter *4*, 1142–1188.

5. Krauskopf, T., Richter, F.H., Zeier, W.G., and Janek, J. (2020). Physicochemical concepts of the lithium metal anode in solid-state batteries. Chem. Rev. *120*, 7745–7794.

6. Lu, Y., Zhao, C.Z., Yuan, H., Cheng, X.B., Huang, J.Q., and Zhang, Q. (2021). Critical current density in solid-state lithium metal batteries: mechanism, influences, and strategies. Adv. Funct. Mater. *31*, 2009925.

7. Kazyak, E., Garcia-Mendez, R., LePage, W.S., Sharafi, A., Davis, A.L., Sanchez, A.J., Chen, K.H., Haslam, C., Sakamoto, J., and Dasgupta, N.P. (2020). Li penetration in ceramic solid electrolytes: operando microscopy analysis of morphology, propagation, and reversibility. Matter *2*, 1025–1048.

8. Huang, Q.-A., Bai, Y., Wang, L., Wang, J., Zhang, F., Wang, L., Li, X., and Zhang, J. (2022). Time-frequency analysis of Li solid-phase diffusion in spherical active particles under typical discharge modes. J. Energy Chem. *67*, 209–224.

9. Osaka, T., Mukoyama, D., and Nara, H. (2015). Review—development of diagnostic process for commercially available batteries, especially lithium ion battery, by electrochemical impedance spectroscopy. J. Electrochem. Soc. *162*, A2529–A2537.

10. Zheng, Y., Shi, Z., Guo, D., Dai, H., and Han, X. (2021). A simplification of the time-domain equivalent circuit model for lithium-ion batteries based on low-frequency electrochemical impedance spectra. J. Power Sources *489*, 229505.

11. Huang, Q.-A., Shen, Y., Huang, Y., Zhang, L., and Zhang, J. (2016). Impedance characteristics and diagnoses of automotive lithium-ion batteries at 7.5% to 93.0% state of charge. Electrochim. Acta *219*, 751–765.

12. Xia, J., Wang, C., Wang, X., Bi, L., and Zhang, Y. (2020). A perspective on DRT applications for the analysis of solid oxide cell electrodes. Electrochim. Acta *349*, 136328.

13. Rashid, M., and Gupta, A. (2015). Effect of relaxation periods over cycling performance of a Li-ion battery. J. Electrochem. Soc. *162*, A3145–A3153.

14. Huang, Q.-A., Hui, R., Wang, B., and Zhang, J. (2007). A review of AC impedance modeling and validation in SOFC diagnosis. Electrochim. Acta *52*, 8144–8164.

15. Wang, J., Huang, Q., Li, W., Wang, J., Zhuang, Q., and Zhang, J. (2020). Fundamentals of distribution of relaxation times for electrochemical impedance spectroscopy. J. Electrochem. *26*, 607–627.

16. Boukamp, B.A. (2020). Distribution (function) of relaxation times, successor to complex nonlinear least squares analysis of electrochemical impedance spectroscopy? J. Phys.: Energy *2*, 042001.

17. Sheng, C., Yu, F., Li, C., Zhang, H., Huang, J., Wu, Y., Armand, M., and Chen, Y. (2021). Diagnosing the SEI layer in a potassium ion battery using distribution of relaxation time. J. Phys. Chem. Lett. *12*, 2064–2071.

18. Steinhauer, M., Risse, S., Wagner, N., and Friedrich, K.A. (2017). Investigation of the solid electrolyte interphase formation at graphite anodes in lithium-ion batteries with electrochemical impedance spectroscopy. Electrochim. Acta *228*, 652–658.

19. Li, L., Fang, C., Wei, W., Zhang, L., Ye, Z., He, G., and Huang, Y. (2020). Nano-ordered structure regulation in delithiated Si anode triggered by homogeneous and stable Li-ion diffusion at the interface. Nano Energy *72*, 104651.

20. Smrekar, S., Bracamonte, M.V., Primo, E.N., Luque, G.L., Thomas, J., Barraco, D.E., and Leiva, E. (2020). A mapping of the physical and electrochemical properties of composite lithium-ion batteries anodes made from graphite, Sn, and Si. Batteries Supercaps *3*, 1248–1256.

21. Chen, L.L., Song, W.L., Li, N., Jiao, H., Han, X., Luo, Y., Wang, M., Chen, H., Jiao, S., and Fang, D. (2020). Nonmetal current collectors: the key component for high-energy-density aluminum batteries. Adv. Mater. *32*, e2001212.

22. Shafiei Sabet, P., Warnecke, A.J., Meier, F., Witzenhausen, H., Martinez-Laserna, E., and Sauer, D.U. (2020). Non-invasive yet separate investigation of anode/cathode degradation of lithium-ion batteries (nickel–cobalt–manganese vs. graphite) due to accelerated aging. J. Power Sources *449*, 227369.

23. Finegan, D.P., Zhu, J., Feng, X., Keyser, M., Ulmefors, M., Li, W., Bazant, M.Z., and Cooper, S.J. (2021). The application of data-driven methods and physics-based learning for improving battery safety. Joule *5*, 316–329.

24. Reichert, M., Andre, D., Rösmann, A., Janssen, P., Bremes, H.G., Sauer, D.U., Passerini, S., and Winter, M. (2013). Influence of relaxation time on the lifetime of commercial lithium-ion cells. J. Power Sources *239*, 45–53.

25. v Schweidler, E.R. (1907). Studien über die Anomalien im Verhalten der Dielektrika. Ann. Phys. *329*, 711–770.

26. Wan, T.H., Saccoccio, M., Chen, C., and Ciucci, F. (2015). Influence of the discretization methods on the distribution of relaxation times deconvolution: implementing radial basis functions with DRTtools. Electrochim. Acta *184*, 483–499.

27. Ciucci, F. (2019). Modeling electrochemical impedance spectroscopy. Curr. Opin. Electrochem. *13*, 132–139.

28. Li, X., Ahmadi, M., Collins, L., and Kalinin, S.V. (2019). Deconvolving distribution of relaxation times, resistances and inductance from electrochemical impedance spectroscopy via statistical model selection: exploiting structural-sparsity regularization and data-driven parameter tuning. Electrochim. Acta *313*, 570–583.

29. Hahn, M., Rosenbach, D., Krimalowski, A., Nazarenus, T., Moos, R., Thelakkat, M., and Danzer, M.A. (2020). Investigating solid polymer and ceramic electrolytes for lithium-ion batteries by means of an extended distribution of relaxation times analysis. Electrochim. Acta *344*, 136060.

30. Boukamp, B.A. (2015). Fourier transform distribution function of relaxation times; application and limitations. Electrochim. Acta *154*, 35–46.

31. Tuncer, E., and Gubanski, S.M. (2001). On dielectric data analysis. Using the Monte Carlo method to obtain relaxation time distribution and comparing non-linear spectral function fits. IEEE Trans. Dielectr. Electr. Insul. *8*, 310–320.

32. Hörlin, T. (1998). Deconvolution and maximum entropy in impedance spectroscopy of noninductive systems. Solid State Ionics *107*, 241–253.

33. Eckert, M., Kölsch, L., and Hohmann, S. (2015). Fractional algebraic identification of the distribution of relaxation times of battery cells. In 2015 54th IEEE Conference on Decision and Control (CDC), pp. 2101–2108.

34. Liu, J., and Ciucci, F. (2020). The Gaussian process distribution of relaxation times: a machine learning tool for the analysis and prediction of electrochemical impedance spectroscopy data. Electrochim. Acta *331*, 135316.

35. Tesler, A.B., Lewin, D.R., Baltianski, S., and Tsur, Y. (2010). Analyzing results of impedance spectroscopy using novel evolutionary programming techniques. J. Electroceram. *24*, 245–260.

36. Schlüter, N., Ernst, S., and Schröder, U. (2020). Direct access to the optimal regularization parameter in distribution of relaxation times analysis. ChemElectroChem *7*, 3445–3458.

37. Hahn, M., Schindler, S., Triebs, L.-C., and Danzer, M.A. (2019). Optimized process parameters for a reproducible distribution of relaxation times analysis of electrochemical systems. Batteries *5*, 43.

38. Zhang, Y., Chen, Y., Li, M., Yan, M., Ni, M., and Xia, C. (2016). A high-precision approach to reconstruct distribution of relaxation times from electrochemical impedance spectroscopy. J. Power Sources *308*, 1–6.

39. Žic, M., Vlašić, L., Subotić, V., Pereverzyev, S., Fajfar, I., and Kunaver, M. (2022). Extraction of distribution function of relaxation times by using Levenberg-Marquardt algorithm: a new approach to apply a discretization error free Jacobian matrix. J. Electrochem. Soc. *169*, 030508.

40. Hershkovitz, S., Tomer, S., Baltianski, S., and Tsur, Y. (2011). ISGP: impedance spectroscopy analysis using evolutionary programming procedure. ECS Trans. *33*, 67–73.

41. Maradesa, A., Py, B., Quattrocchi, E., and Ciucci, F. (2022). The probabilistic deconvolution of the distribution of relaxation times with finite Gaussian processes. Electrochim. Acta *413*, 140119.

42. Hong, J., Bhardwaj, A., Bae, H., Kim, I.-h., and Song, S.-J. (2020). Electrochemical impedance analysis of SOFC with transmission line model using distribution of relaxation times (DRT). J. Electrochem. Soc. *167*, 114504.

43. Lenser, C., and Menzler, N.H. (2019). Impedance characterization of supported oxygen ion conducting electrolytes. Solid State Ionics *334*, 70–81.

44. Tang, Z., Huang, Q.-A., Wang, Y.-J., Zhang, F., Li, W., Li, A., Zhang, L., and Zhang, J. (2020). Recent progress in the use of electrochemical impedance spectroscopy for the measurement, monitoring, diagnosis and optimization of proton exchange membrane fuel cell performance. J. Power Sources *468*, 228361.

45. Guo, D., Yang, G., Zhao, G., Yi, M., Feng, X., Han, X., Lu, L., and Ouyang, M. (2020). Determination of the differential capacity of lithium-ion batteries by the deconvolution of electrochemical impedance spectra. Energies *13*, 915.

46. Song, J., and Bazant, M.Z. (2018). Electrochemical impedance imaging via the distribution of diffusion times. Phys. Rev. Lett. *120*, 116001.

47. Schönleber, M., and Ivers-Tiffée, E. (2015). The distribution function of differential capacity as a new tool for analyzing the capacitive properties of lithium-ion batteries. Electrochem. Commun. *61*, 45–48.

48. Quattrocchi, E., Wan, T.H., Curcio, A., Pepe, S., Effat, M.B., and Ciucci, F. (2019). A general model for the impedance of batteries and supercapacitors: the non-linear distribution of diffusion times. Electrochim. Acta *324*, 134853.

49. Wang, Q., Hu, Z., Xu, L., Li, J., Gan, Q., Du, X., and Ouyang, M. (2021). A comparative study of equivalent circuit model and distribution of relaxation times for fuel cell impedance diagnosis. Int. J. Energy Res. *45*, 15948–15961.

50. Huang, J., Li, Z., Liaw, B.Y., and Zhang, J. (2016). Graphical analysis of electrochemical impedance spectroscopy data in Bode and Nyquist representations. J. Power Sources *309*, 82–98.

51. Kim, S.J., Choi, M.-B., Park, M., Kim, H., Son, J.-W., Lee, J.-H., Kim, B.-K., Lee, H.-W., Kim, S.-G., and Yoon, K.J. (2017). Acceleration tests: degradation of anode-supported planar solid oxide fuel cells at elevated operating temperatures. J. Power Sources *360*, 284–293.

52. Weiß, A., Schindler, S., Galbiati, S., Danzer, M.A., and Zeis, R. (2017). Distribution of relaxation times analysis of high-temperature PEM fuel cell impedance spectra. Electrochim. Acta *230*, 391–398.

53. Liu, J., Wan, T.H., and Ciucci, F. (2020). A Bayesian view on the Hilbert transform and the Kramers-Kronig transform of electrochemical impedance data: probabilistic estimates and quality scores. Electrochim. Acta *357*, 136864.

54. Boukamp, B.A. (1995). A linear Kronig-Kramers transform test for immittance data validation. J. Electrochem. Soc. *142*, 1885–1894.

55. Ciucci, F. (2020). The Gaussian process Hilbert transform (GP-HT): testing the consistency of electrochemical impedance spectroscopy data. J. Electrochem. Soc. *167*, 126503.

56. Agarwal, P., Orazem, M.E., and Garcia-Rubio, L.H. (1995). Application of measurement models to impedance spectroscopy: III. Evaluation of consistency with the Kramers-Kronig relations. J. Electrochem. Soc. *142*, 4159–4168.

57. Boukamp, B.A. (1993). Practical application of the Kramers-Kronig transformation on impedance measurements in solid state electrochemistry. Solid State Ionics *62*, 131–141.

58. Schönleber, M., Klotz, D., and Ivers-Tiffée, E. (2014). A method for improving the robustness of linear Kramers-Kronig validity tests. Electrochim. Acta *131*, 20–27.

59. Schmidt, J.P., Chrobak, T., Ender, M., Illig, J., Klotz, D., and Ivers-Tiffée, E. (2011). Studies on $LiFePO_4$ as cathode material using impedance spectroscopy. J. Power Sources *196*, 5342–5348.

60. Danzer, M.A. (2019). Generalized distribution of relaxation times analysis for the characterization of impedance spectra. Batteries *5*, 53.

61. Saccoccio, M., Wan, T.H., Chen, C., and Ciucci, F. (2014). Optimal regularization in distribution of relaxation times applied to electrochemical impedance spectroscopy: ridge and Lasso regression methods—a theoretical and experimental study. Electrochim. Acta *147*, 470–482.

62. Hansen, P.C., and O'Leary, D.P. (1993). The use of the L-curve in the regularization of discrete ill-posed problems. SIAM J. Sci. Comput. *14*, 1487–1503.

63. Schlüter, N., Ernst, S., and Schröder, U. (2019). Finding the optimal regularization parameter in distribution of relaxation times analysis. ChemElectroChem *6*, 6027–6037.

64. Melo, B.M.G., Loureiro, F.J.A., Fagg, D.P., Costa, L.C., and Graça, M.P.F. (2021). DFRTtoEIS: an easy approach to verify the consistency of a DFRT generated from an impedance spectrum. Electrochim. Acta *366*, 137429.

65. Lu, Y., Zhao, C.-Z., Zhang, R., Yuan, H., Hou, L.-P., Fu, Z.-H., Chen, X., Huang, J.-Q., and Zhang, Q. (2021). The carrier transition from Li atoms to Li vacancies in solid-state lithium alloy anodes. Sci. Adv. *7*, eabi5520.

66. Chen, X., Li, L., Liu, M., Huang, T., and Yu, A. (2021). Detection of lithium plating in lithium-ion batteries by distribution of relaxation times. J. Power Sources *496*, 229867.

67. Song, Y.-W., Peng, Y.-Q., Zhao, M., Lu, Y., Liu, J.-N., Li, B.-Q., and Zhang, Q. (2021). Understanding the impedance response of lithium polysulfide symmetric cells. Small Sci. *1*, 2100042.

68. Yu, S., Mertens, A., Tempel, H., Schierholz, R., Kungl, H., and Eichel, R.A. (2018). Monolithic all-phosphate solid-state lithium-ion battery with improved interfacial compatibility. ACS Appl. Mater. Interfaces *10*, 22264–22277.

69. Lu, Y., Huang, X., Ruan, Y., Wang, Q., Kun, R., Yang, J., and Wen, Z. (2018). An *in situ* element permeation constructed high endurance Li–LLZO interface at high current densities. J. Mater. Chem. A *6*, 18853–18858.

70. Van der Ven, A., Bhattacharya, J., and Belak, A.A. (2013). Understanding Li diffusion in Li-intercalation compounds. Acc. Chem. Res. *46*, 1216–1225.

71. Zhu, J., Knapp, M., Liu, X., Yan, P., Dai, H., Wei, X., and Ehrenberg, H. (2020). Low-temperature separating lithium-ion battery interfacial polarization based on distribution of relaxation times (DRT) of impedance. IEEE Trans. Transp. Electrific. *7*, 410–421.

72. Zhou, X., Huang, J., Pan, Z., and Ouyang, M. (2019). Impedance characterization of lithium-ion batteries aging under high-temperature cycling: importance of electrolyte-phase diffusion. J. Power Sources *426*, 216–222.

73. Huang, X., Lu, Y., Song, Z., Rui, K., Wang, Q., Xiu, T., Badding, M.E., and Wen, Z. (2019). Manipulating Li_2O atmosphere for sintering dense $Li_7La_3Zr_2O_{12}$ solid electrolyte. Energy Storage Mater. *22*, 207–217.

74. Huang, X., Wu, L., Huang, Z., Lin, J., and Xu, X. (2020). Characterization and testing of key electrical and electrochemical properties of lithium-ion solid electrolytes. Energy Storage Sci. Technol. *9*, 479–500.

75. Zhuang, L.B., Huang, X., Lu, Y., Tang, J.W., Zhou, Y.J., Ao, X., Yang, Y., and Tian, B.B. (2021). Phase transformation and grain-boundary segregation in Al-Doped $Li_7La_3Zr_2O_{12}$ ceramics. Ceram. Int. *47*, 22768–22775.

76. Wang, Q., Lu, Y., Jin, J., Chen, C., and Wen, Z. (2020). $Li_{1.5}Al_{0.5}Ge_{1.5}(PO_4)_3$ ceramic based lithium-sulfur batteries with high cycling stability enabled by a dual confinement effect for polysulfides. ChemElectroChem *7*, 4093–4100.

77. Ma, C., Chen, K., Liang, C., Nan, C.-W., Ishikawa, R., More, K., and Chi, M. (2014). Atomic-scale origin of the large grain-boundary resistance in perovskite Li-ion-conducting solid electrolytes. Energy Environ. Sci. *7*, 1638.

78. Busche, M.R., Weiss, M., Leichtweiss, T., Fiedler, C., Drossel, T., Geiss, M., Kronenberger, A., Weber, D.A., and Janek, J. (2020). The formation of the solid/liquid electrolyte interphase (SLEI) on NASICON-type glass ceramics and LiPON. Adv. Mater. Interfaces *7*, 2000380.

79. Jia, H., Gao, P., Zou, L., Han, K.S., Engelhard, M.H., He, Y., Zhang, X., Zhao, W., Yi, R., Wang, H., et al. (2020). Controlling ion coordination structure and diffusion kinetics for optimized electrode-electrolyte interphases and high-performance Si anodes. Chem. Mater. *32*, 8956–8964.

80. Risse, S., Cañas, N.A., Wagner, N., Härk, E., Ballauff, M., and Friedrich, K.A. (2016). Correlation of capacity fading processes and electrochemical impedance spectra in lithium/sulfur cells. J. Power Sources *323*, 107–114.

81. Risse, S., Härk, E., Kent, B., and Ballauff, M. (2019). Operando analysis of a lithium/sulfur battery by small-angle neutron scattering. ACS Nano *13*, 10233–10241.

82. Dollé, M., Orsini, F., Gozdz, A.S., and Tarascon, J.M. (2001). Development of reliable three-electrode impedance measurements in plastic Li-ion batteries. J. Electrochem. Soc. *148*, A851–A857.

83. Shafiei Sabet, P., Stahl, G., and Sauer, D.U. (2020). Non-invasive investigation of predominant processes in the impedance spectra of high energy lithium-ion batteries with nickel–cobalt–aluminum cathodes. J. Power Sources *472*, 228189.

84. Shafiei Sabet, P., and Sauer, D.U. (2019). Separation of predominant processes in electrochemical impedance spectra of lithium-ion batteries with nickel-manganese-cobalt cathodes. J. Power Sources *425*, 121–129.

85. Shu, C., Wu, C., Long, J., Guo, H., Dou, S.-X., and Wang, J. (2019). Highly reversible Li-O_2 battery induced by modulating local electronic structure via synergistic interfacial interaction between ruthenium nanoparticles and hierarchically porous carbon. Nano Energy *57*, 166–175.

86. Pesci, F.M., Bertei, A., Brugge, R.H., Emge, S.P., Hekselman, A.K.O., Marbella, L.E., Grey, C.P., and Aguadero, A. (2020). Establishing ultralow activation energies for lithium transport in garnet electrolytes. ACS Appl. Mater. Interfaces *12*, 32806–32816.

87. Mariappan, C.R., Yada, C., Rosciano, F., and Roling, B. (2011). Correlation between micro-structural properties and ionic conductivity of $Li_{1.5}Al_{0.5}Ge_{1.5}(PO_4)_3$ ceramics. J. Power Sources *196*, 6456–6464.

88. Huang, B., Yao, X., Huang, Z., Guan, Y., Jin, Y., and Xu, X. (2015). Li_3PO_4 -doped $Li_7P_3S_{11}$ glass-ceramic electrolytes with enhanced lithium ion conductivities and application in

all-solid-state batteries. J. Power Sources *284*, 206–211.

89. Yu, C., van Eijck, L., Ganapathy, S., and Wagemaker, M. (2016). Synthesis, structure and electrochemical performance of the argyrodite Li_6PS_5Cl solid electrolyte for Li-ion solid state batteries. Electrochim. Acta *215*, 93–99.

90. Katzer, F., and Danzer, M.A. (2021). Analysis and detection of lithium deposition after fast charging of lithium-ion batteries by investigating the impedance relaxation. J. Power Sources *503*, 230009.

91. Müller, M., Schmieg, J., Dierickx, S., Joos, J., Weber, A., Gerthsen, D., and Ivers-Tiffée, E. (2022). Reducing impedance at a Li-metal anode/garnet-type electrolyte interface implementing chemically resolvable in layers. ACS Appl. Mater. Interfaces *14*, 14739–14752.

92. Soni, R., Robinson, J.B., Shearing, P.R., Brett, D.J.L., Rettie, A.J.E., and Miller, T.S. (2022). Quantitative deconvolution of electrode processes in lithium-sulfur batteries through distribution of relaxation times. SSRN Journal. https://doi.org/10.2139/ssrn.4030055.

93. Clematis, D., Ferrari, T., Bertei, A., Asensio, A.M., Carpanese, M.P., Nicolella, C., and Barbucci, A. (2021). On the stabilization and extension of the distribution of relaxation times analysis. Electrochim. Acta *391*, 138916.

94. Lu, Y., Gu, S., Guo, J., Rui, K., Chen, C., Zhang, S., Jin, J., Yang, J., and Wen, Z. (2017). Sulfonic groups originated dual-functional interlayer for high performance lithium-sulfur battery. ACS Appl. Mater. Interfaces *9*, 14878–14888.

95. Lu, Y., Gu, S., Hong, X., Rui, K., Huang, X., Jin, J., Chen, C., Yang, J., and Wen, Z. (2018). Pre-modified Li_3PS_4 based interphase for lithium anode towards high-performance Li–S battery. Energy Storage Mater. *11*, 16–23.

96. Lu, Y., Huang, X., Song, Z., Rui, K., Wang, Q., Gu, S., Yang, J., Xiu, T., Badding, M.E., and Wen, Z. (2018). Highly stable garnet solid electrolyte based Li–S battery with modified anodic and cathodic interfaces. Energy Storage Mater. *15*, 282–290.

97. Yan, C., Jiang, L.L., Yao, Y.X., Lu, Y., Huang, J.Q., and Zhang, Q. (2021). Nucleation and growth mechanism of anion-derived solid electrolyte interphase in rechargeable batteries. Angew. Chem. Int. Ed. Engl. *60*, 8521–8525.

98. Medvedev, D. (2020). Distribution of relaxation time analysis for solid state electrochemistry. Electrochim. Acta *360*, 137034.

99. Zhang, F., Huang, Q.-A., Tang, Z., Li, A., Shao, Q., Zhang, L., Li, X., and Zhang, J. (2020). A review of mechanics-related material damages in all-solid-state batteries: mechanisms, performance impacts and mitigation strategies. Nano Energy *70*, 104545.

100. Heins, T.P., Leithoff, R., Schlüter, N., Schröder, U., and Dröder, K. (2020). Impedance spectroscopic investigation of the impact of erroneous cell assembly on the aging of lithium-ion batteries. Energy Technol *8*, 1900288.

101. Ashuri, M., Golmohammad, M., Soleimany Mehranjani, A., and Faghihi Sani, M. (2021). Al-doped $Li_7La_3Zr_2O_{12}$ garnet-type solid electrolytes for solid-state Li-Ion batteries. J. Mater. Sci Mater. Electron. *32*, 6369–6378.

102. Li, S., Li, Z., Huai, L., Ma, M., Luo, K., Chen, J., Wang, D., and Peng, Z. (2021). A strongly interactive adatom/substrate interface for dendrite-free and high-rate Li metal anodes. J. Energy Chem. *62*, 179–190.

103. Rosenbach, D., Mödl, N., Hahn, M., Petry, J., Danzer, M.A., and Thelakkat, M. (2019). Synthesis and comparative studies of solvent-free brush polymer electrolytes for lithium batteries. ACS Appl. Energy Mater. *2*, 3373–3388.

104. Liu, J., and Ciucci, F. (2020). The deep-prior distribution of relaxation times. J. Electrochem. Soc. *167*, 026506.

105. Kulikovsky, A. (2020). PEM fuel cell distribution of relaxation times: a method for the calculation and behavior of an oxygen transport peak. Phys. Chem. Chem. Phys. *22*, 19131–19138.

106. Hershkovitz, S., Baltianski, S., and Tsur, Y. (2011). Harnessing evolutionary programming for impedance spectroscopy analysis: a case study of mixed ionic-electronic conductors. Solid State Ionics *188*, 104–109.

107. Žic, M., and Pereverzyev, S., Jr. (2018). Adaptive multi-parameter regularization in electrochemical impedance spectroscopy. https://www.ricam.oeaw.ac.at/files/reports/18/rep18-16.pdf.

108. Žic, M., Pereverzyev, S., Jr., Subotić, V., and Pereverzyev, S. (2020). Adaptive multi-parameter regularization approach to construct the distribution function of relaxation times. GEM *11*, 2.

109. Quattrocchi, E., Wan, T.H., Belotti, A., Kim, D., Pepe, S., Kalinin, S.V., Ahmadi, M., and Ciucci, F. (2021). The deep-DRT: A deep neural network approach to deconvolve the distribution of relaxation times from multidimensional electrochemical impedance spectroscopy data. Electrochim. Acta *392*, 139010.

110. Mertens, A., and Granwehr, J. (2017). Two-dimensional impedance data analysis by the distribution of relaxation times. J. Energy Storage *13*, 401–408.

111. Kim, D., Muckley, E.S., Creange, N., Wan, T.H., Ann, M.H., Quattrocchi, E., Vasudevan, R.K., Kim, J.H., Ciucci, F., Ivanov, I.N., et al. (2021). Exploring transport behavior in hybrid perovskites solar cells via machine learning analysis of environmental-dependent impedance spectroscopy. Adv. Sci. (Weinh) *8*, e2002510.

112. Jiang, B.B., Gent, W.E., Mohr, F., Das, S., Berliner, M.D., Forsuelo, M., Zhao, H., Attia, P.M., Grover, A., Herring, P.K., et al. (2021). Bayesian learning for rapid prediction of lithium-ion battery-cycling protocols. Joule *5*, 3187–3203.

113. Lai, X., Huang, Y., Deng, C., Gu, H., Han, X., Zheng, Y., and Ouyang, M. (2021). Sorting, regrouping, and echelon utilization of the large-scale retired lithium batteries: a critical review. Renew. Sustain. Energy Rev. *146*, 111162.

114. Lai, X., Huang, Y., Gu, H., Deng, C., Han, X., Feng, X., and Zheng, Y. (2021). Turning waste into wealth: a systematic review on echelon utilization and material recycling of retired lithium-ion batteries. Energy Storage Mater. *40*, 96–123.

115. Xu, L., Yang, Y., Xiao, Y., Cai, W.-L., Yao, Y.-X., Chen, X.-R., Yan, C., Yuan, H., and Huang, J.-Q. (2022). In-situ determination of onset lithium plating for safe Li-ion batteries. J. Energy Chem. *67*, 255–262.

116. Wang, J., Huang, Q.-A., Li, W., Wang, J., Bai, Y., Zhao, Y., Li, X., and Zhang, J. (2022). Insight into the origin of pseudo peaks decoded by the distribution of relaxation times/differential capacity method for electrochemical impedance spectroscopy. J. Electroanal. Chem. *910*, 116176.